Prediction Regions for Interval-valued Time Series[1]

Gloria GONZÁLEZ-RIVERA[2]

and

Yun LUO

Department of Economics
University of California, Riverside, CA, USA

Esther RUIZ

Department of Statistics
Universidad Carlos III de Madrid, Spain

October 4, 2018

[1]We are grateful to participants in the International Symposium on Forecasting in Cairns 2017 and in the 2nd International Symposium on Interval Data Modeling, Xiamen University for useful comments. Gloria González-Rivera acknowledges financial support from the 2015/2016 Chair of Excellence UC3M/Banco de Santander and the UC-Riverside Academic Senate grants. Esther Ruiz and Gloria González-Rivera are grateful to the Spanish Government contract grant ECO2015-70331-C2-2-R (MINECO/FEDER).

[2]Corresponding author: gloria.gonzalez@ucr.edu, (951) 827-1590

Abstract

We approximate probabilistic forecasts for interval-valued time series by offering alternative approaches to construct bivariate prediction regions of the interval center and range (or lower/upper bounds). We estimate a bivariate system of the center/log-range, which may not be normally distributed. Implementing analytical or bootstrap methods, we directly transform prediction regions for center/log-range into those for center/range and upper/lower bounds systems. We propose new metrics to evaluate the regions performance. Monte Carlo simulations show bootstrap methods being preferred even in Gaussian systems. For daily SP500 low/high return intervals, we build joint conditional prediction regions of the return level and return volatility.

Key Words: Bootstrap, Constraint Regression, Coverage Rates, Logarithmic Transformation, QML estimation.

JEL Classification: C01, C22, C53

1 Introduction

Data sets in interval format are common in many disciplines. See Blanco-Fernández and Winker (2016) for different data generation mechanisms of interval data. In economics, we have many examples. For instance, in stock markets, it is standard to provide the daily interval of low/high asset prices. In bond markets, traders report bid/ask intervals. In energy markets, the US Energy Information Administration provides min/max retail prices of electricity at the state level. The US Department of Agriculture also provides daily low and high prices on agricultural commodities and livestock. In earth sciences, temperatures are also recorded in the min/max format. It should be noted that in many instances, the interval format is the only available format to the researcher. There are several reasons to prefer interval records. For instance, in stock markets it is customary to report the daily closing price, which is just one-point measurement, while we observe plenty of price points over the trading day. Other records, like an average temperature or like those provided by USDA as daily weighted average prices on commodities and livestock, are not very informative to market participants. In other instances in which the data is sensitive to privacy concerns such as income reporting, the records must be aggregated, e.g. income intervals.

Our interest is in interval-valued times series defined as a collection of interval realizations ordered over time, i.e., $\{(y_{l,t}, y_{u,t})\}$ for $t = 1, ...T$, where $y_{l,t}$ is the lower bound and $y_{u,t}$ is the upper bound of the interval at time t, such that $y_{l,t} \leq y_{u,t}$ for all t. An equivalent representation is given by considering the center of the interval $C_t = (y_{l,t} + y_{u,t})/2$ and the range $R_t = y_{u,t} - y_{l,t} \geq 0$, i.e., $\{(C_t, R_t)\}$ for $t = 1, ...T$. Most of the econometric analysis in this area has focused on model estimation and inference, and though it is possible to construct point forecasts based on a given model or algorithm, the question of constructing probabilistic forecasts for interval data has not been addressed yet. This is the main question that we aim to analyze in this paper. There are several routes to construct a probabilistic forecast for the lower/upper bounds system or for the center/range system, which involve some trade-offs between estimation and prediction decisions.

When dealing with lower/upper bounds systems, one needs to incorporate the constraint $y_{l,t} \leq y_{u,t}$ into the estimation. González-Rivera and Lin (2013) propose a two-step estimator (Maximum Likelihood (ML) and Least Squares (LS)) and a modified two-step estimator (ML and Minimum Distance) based on assuming a truncated bivariate normal density of the errors of the lower/upper bounds system. The estimation of the system is complex but it is possible to construct a direct bivariate density forecast for the upper/lower bounds, if the truncated bivariate normal density is the right assumption. Alternatively, dealing with the center/range system, one needs to incorporate the constraint $R_t \geq 0$. Lima Neto and De Carvalho (2010) impose non-negative constraints on the parameters of the range equation, which are unnecessarily too restrictive and complicate the estimation of the system. Tu and Wang (2016) overcome the restriction $R_t \geq 0$ by log-transforming the range, and estimating the center/log-range system without imposing any distributional assumptions. However, forecasting the center/range or lower/upper bounds will be more complicated. First, for point forecasts, one needs the inverse transformation, i.e. $R_t = \exp[\log R_t]$, which itself introduces non-trivial econometric issues. Secondly, for a density forecast, a joint distributional assumption for the center and range or for the upper and lower bounds is required.

In this paper, we contribute to the literature by approximating a probabilistic forecast for interval-valued time series. We offer alternative approaches to construct bivariate forecast regions of the center and the range (or lower and upper bounds) of the interval. We will start with a dynamic model for the center/log-range system. We specify a VAR system to be estimated by quasi-maximum likelihood (QML), maximizing a bivariate Gaussian density, that guarantees the consistency of the estimators.[1] We estimate only the center/log-range system, construct prediction regions for this system, and based on these estimates, construct prediction regions for the center/range system and for the upper/lower bounds system. We implement analytical and numerical

[1]Tu and Wang (2016) used the estimator of Yao and Zhao (2013) that relies on kernel estimates of the likelihood. This estimator is computationally more demanding than QML and depends on the choice of tuning parameters. Their empirical results suggest that both estimators are very similar and, consequently, we focus on the QML estimator.

approaches to move a prediction region for the center/log-range system to prediction regions for the other systems. If the center/log-range system is bivariate normally distributed, we obtain analytical forecast ellipsoids with a desired probability coverage. Furthermore, as proposed by Lutkephol (1991), we could also construct forecast regions by using Bonferroni rectangles, which are simpler and rather popular among practitioners. However, the center and/or the log-range are often not normally distributed and the joint system will not be bivariate normal. In these cases, we obtain forecasts of the center/log-range system using the bootstrap procedure proposed by Fresoli et al. (2015) for VAR models, which does not require any specific assumption on the forecast error distribution. After obtaining bootstrap replicates of future values of the center/log-range system, we construct forecast regions as ellipsoids, Bonferroni rectangles, or using the Tukey peeling. Implementing either analytical or bootstrap methods, the prediction regions constructed for the center/log-range system can be directly transformed into prediction regions for the center/range system. For instance, consider a normal ellipse with $(1-\alpha)\%$ probability coverage. The boundary of this ellipse is the $(1-\alpha)\%$ bivariate quantile. Its boundary points (center, log-range) can be transformed into another boundary of points (center, exp(log-range)) of a prediction region for the center/range system. The new region will not preserve the shape of an ellipse but it will have the same coverage because the exponential function is a monotonic transformation. An important advantage of our approach is that, by focusing on prediction regions rather than on point forecasts, we avoid the biases that are associated with the exp-transformation of the point forecasts of log-transformed variables, for which a bias correction is necessary to obtain the conditional mean of the variable of interest[2]; see, for example, Granger and Newbold (1976) and Guerrero (1993).

We compare the performance of the prediction regions considered in this paper according to sev-

[2]For point forecasts of Gaussian VAR models, Ariño and Franses (2000) and Bardsen and Lutkepohl (2011) give explicit expressions for the optimal point forecasts of the levels when both variables are log-transformed. Furthermore, Bardsen and Lutkepohl (2011) show that, despite its theoretical advantages, optimal point forecasts are inferior to naive forecasts if specification and estimation uncertainty are taken into account. Hence, they conclude that, in practice when the interest is a point forecast, using the exponential of the log-forecasts is preferable to using the optimal forecasts; see also Mayr and Ulbricht (2015) for an empirical application to forecasting GDP. Finally, it is important to point out that the optimal transformations are not designed to obtain density forecasts.

eral metrics. The most basic required property is coverage so that regions are reliable when the empirical coverage is close to the nominal coverage. Beyond coverage, the literature on evaluating multivariate prediction regions is rather thin. To our knowledge, there is one additional metric that brings the volume of the region to interact with its coverage (Golestaneh *et al.*, 2017). In this paper, we also contribute to this literature by introducing several new measures that account for (i) the location of out-of-the-region points with respect to a central point of the region, (ii) the tightness of the intervals that result from projecting the two-dimensional region into one-dimensional intervals, and (iii) the distance of the also projected out-of-the-region points to the projected one-dimensional interval. These new measures bring a notion of risk associated with the prediction region. In addition, we also provide a description of the distribution of the out-of-the-region points around the region to measure whether the region is probability-centered.

For the three systems (center/log-range, center/range, and upper/lower bounds), we perform several Monte Carlo simulations to assess the out-of-sample performance of the prediction regions constructed with analytical and bootstrap methods. We evaluate bivariate Gaussian and non-Gaussian center/log-range systems and their implied distributions for the center/range and upper/lower bounds systems. We note that even for Gaussian systems, bootstrap methods to construct ellipsoids and Bonferroni rectangles deliver the best performance, mainly when the estimation sample is small and estimation uncertainty is most relevant. For non-Gaussian systems, the performance depends on whether the joint distribution of the center/log-range system is symmetric or not. If symmetry is present, bootstrap ellipsoids and their transformations are recommended. For asymmetric non-Gaussian systems, bootstrap Bonferroni rectangles are preferred.

Using the analytical and bootstrap procedures described above, we construct forecast regions for a time series of daily low/high return intervals of the SP500 index. These intervals are more informative than just a daily one-point measurement (end-of-day return) as they encompass all returns during the day. There are commonalities between the analysis of return intervals and the

standard analysis of end-of-the-day returns and their volatility. The center of the return interval has large kurtosis and does not have any autocorrelation. The log-range, which is close to be normally distributed, is a proxy for volatility as proposed by Parkinson (1980) and Alizadeh *et al.* (2002). It shows a strong autocorrelation as that of an autoregressive process, which is similar to the patterns found in ARCH and stochastic volatility processes. We also find that there is Granger-causality from the center of the interval to the log-range such that positive and large changes in the center will predict narrower ranges, which is similar to the so-called leverage effect. However, an important difference pertains to the construction of the forecasts. In standard ARCH and stochastic volatility processes, the forecast of the return is mostly zero and together with a forecast of the conditional volatility and some conditional distribution of the return, it is possible to generate a density forecast of future returns. In the interval approach, we forecast jointly the future low/high return interval and construct prediction regions of the center and range of the interval at any desired horizon that do not require parametric distributional assumptions. Overall, the main advantage of the interval approach is that allows for the modeling of the joint conditional density of the return level and the return volatility, which in our sample are contemporaneous and negatively correlated, and consequently allows for the construction of bivariate density forecasts.

The organization of the paper is as follows. In section 2, we establish notation by describing the VAR model for the center/log-range system, its estimation and construction of point forecasts. In section 3, we present analytical prediction regions for a Gaussian center/log-range system and how they translate into those for the center/range and upper/lower bounds systems. In section 4, we introduce bootstrap procedures to deal with prediction regions for non-Gaussian center/log-range systems and their implications for those regions in the center/range and upper/lower bounds systems. In section 5, we propose several new metrics to evaluate the performance of the different prediction regions. In section 6, we report Monte Carlo simulations to compare the performance of the proposed procedures to construct forecast regions. In section 7, we model the SP500 low/high return interval and construct several prediction regions for the interval. We conclude in section 8.

2 The Center/Log-Range System

Even if the final goal is to obtain probabilistic forecasts of the center/range or lower/upper bounds systems, we start by estimating a dynamic model for the center/log-range system that is not subject to any restriction as we are log-transforming the range. We consider a linear bivariate VAR(p) for the center/log-range system from which we will construct a probabilistic forecast for $(C_t, \log R_t)$. Let us call $y_{c,t} \equiv C_t$ and $y_{r,t} \equiv \log R_t$. The bivariate VAR(p) is given by

$$y_{c,t} = \alpha_1 + \sum_{i=1}^{p} \beta_{11}^{(i)} y_{c,t-i} + \sum_{i=1}^{p} \beta_{12}^{(i)} y_{r,t-i} + \varepsilon_{c,t} \tag{2.1}$$

$$y_{r,t} = \alpha_2 + \sum_{i=1}^{p} \beta_{21}^{(i)} y_{c,t-i} + \sum_{i=1}^{p} \beta_{22}^{(i)} y_{r,t-i} + \varepsilon_{r,t} \tag{2.2}$$

where the components of the error vector $(\varepsilon_{c,t}, \varepsilon_{r,t})'$ are white noise processes, possibly contemporaneous correlated, with covariance matrix Ω. The estimation of the parameters of the VAR(p) model proceeds by LS, which is consistent under mild assumptions. The LS estimator is a full information ML estimator when the errors have a bivariate normal distribution. Otherwise, if the errors are non-normal, a QML estimator based on maximizing the Gaussian likelihood will be equivalent to a LS estimator. Let $\theta \equiv (\alpha_1, \alpha_2, \beta_{11}^{(1)}, ..., \beta_{11}^{(p)}, \beta_{12}^{(1)}, ..., \beta_{12}^{(p)}, \beta_{21}^{(1)}, ..., \beta_{21}^{(p)}, \beta_{22}^{(1)}, ..., \beta_{22}^{(p)})$ be the parameter vector to estimate. Following White (1982), the asymptotic distribution of the Gaussian QML estimator is $\sqrt{T}(\hat{\theta} - \theta) \xrightarrow{d} N(0, A^{-1}BA^{-1})$ where matrix A is the (minus) expectation of the Hessian and matrix B is the expectation of the outer product of the score of a Gaussian log-likelihood function. The QML environment will be the most common estimation approach given that bivariate normality of $(\varepsilon_{c,t}, \varepsilon_{r,t})'$ is difficult to entertain. To guarantee bivariate normality of the system, the conditional densities as well as the marginal densities must also be normal density functions. For financial data, there is evidence that the log-range $y_{r,t}$ (as a proxy for volatility) is near-normal (Alizadeh *et al.*, 2002). However, the center $y_{c,t}$ is less likely to be normally distributed because the prevalence of fat tails, at least in financial data at a relative high

frequency, e.g. daily financial returns. In the empirical section, we will test the assumption of bivariate normality as a starting step to construct density forecasts of the full system.

Given an information set available at time T, if the loss function is quadratic, the optimal h-step-ahead point forecasts of the system $(y_{c,t}, y_{r,t})$ are the conditional means denoted by $y_{c,T+h|T}$ and $y_{r,T+h|T}$. Since the VAR(p) model is always invertible, the conditional mean is a linear function of the observations. Therefore, point forecasts of the center and log-range are given by

$$y_{c,T+h|T} = \alpha_1 + \sum_{i=1}^{p} \beta_{11}^{(i)} y_{c,T+h-i|T} + \sum_{i=1}^{p} \beta_{12}^{(i)} y_{r,T+h-i|T} \tag{2.3}$$

$$y_{r,T+h|T} = \alpha_2 + \sum_{i=1}^{p} \beta_{21}^{(i)} y_{c,T+h-i|T} + \sum_{i=1}^{p} \beta_{22}^{(i)} y_{r,T+h-i|T} \tag{2.4}$$

where $y_{c,T+h-i|T} = y_{c,T+h-i}$ and $y_{r,T+h-i|T} = y_{r,T+h-i}$ for $i \geq h$. The corresponding forecast error vector is $(e_{c,T+h|T}, e_{r,T+h|T}) = (y_{c,T+h} - y_{c,T+h|T}, y_{r,T+h} - y_{r,T+h|T})$ with variance-covariance matrix $W_h = \Omega + \sum_{i=1}^{h-1} \Psi_i \Omega \Psi_i'$ where matrices Ψ_i come from the MA(∞) representation of the VAR(p) model. In practice, we plug in consistent estimates, i.e. $\hat{\theta}, \hat{\Omega}$, and $\hat{\Psi}_i$, in the VAR(p) to obtain the estimated h-step-ahead point forecasts and their estimated variance-covariance matrices that are denoted by $\hat{y}_{c,T+h|T}$, $\hat{y}_{r,T+h|T}$, and $\hat{W}_h$ respectively.

If the center/log-range system is bivariate normal, then pointwise bivariate density forecasts can be obtained as follows,

$$\begin{bmatrix} y_{c,T+h} \\ y_{r,T+h} \end{bmatrix} \rightarrow N\Big(\begin{bmatrix} \hat{y}_{c,T+h|T} \\ \hat{y}_{r,T+h|T} \end{bmatrix}, \begin{bmatrix} \hat{W}_{h,11} & \hat{W}_{h,12} \\ \hat{W}_{h,21} & \hat{W}_{h,22} \end{bmatrix} \Big) \tag{2.5}$$

Note that the variance-covariance matrices of the forecast densities in (2.5) do not incorporate parameter uncertainty, which will be negligible when the sample size T is large relative to the number of estimated parameters. When the center/log-range system is non-Gaussian, we can obtain bootstrap pointwise forecast densities by implementing the bootstrap procedure proposed

by Fresoli, Ruiz, and Pascual (2015), which will be described in the forthcoming section 4. The bootstrap forecast densities incorporate parameter uncertainty without relying on any specific forecast error distribution. Even in the Gaussian case, if the estimation sample is not very large, the effect of parameter uncertainty on the forecast may not vanished, and so the use of bootstrap forecast densities may be desired.

3 Gaussian Center/Log-Range System

3.1 Prediction regions for the center/log-range system

Using the forecast densities in (2.5), we can construct pointwise h-step-ahead forecast regions. The $100 \times (1-\alpha)\%$ h-step-ahead forecast ellipsoid for $Y_{T+h} \equiv (y_{c,T+h}, y_{r,T+h})'$ is given by

$$NE_{T+h} = \left[Y_{T+h} | (Y_{T+h} - \hat{Y}_{T+h|T})' \hat{W}_h^{-1} [Y_{T+h} - \hat{Y}_{T+h|T}]\right] \leq q_{1-\alpha}, \tag{3.1}$$

where $q_{1-\alpha}$ is the $(1-\alpha)$ quantile of the chi-square distribution with 2 degrees of freedom. The ellipse is a countour of the bivariate normal center/log-range system with $100 \times (1-\alpha)\%$ coverage.

A straightforward and easy to construct h-step-ahead forecast region is a Bonferroni rectangle with (at least) $100 \times (1-\alpha)\%$ coverage. This rectangle will have the following sides

$$\left[b_{c,\alpha/4}, b_{c,1-\alpha/4}\right] \equiv \left[\hat{y}_{c,T+h|T} - z_{\alpha/4}\sqrt{\hat{W}_{h,11}}, \quad \hat{y}_{c,T+h|T} + z_{\alpha/4}\sqrt{\hat{W}_{h,11}}\right] \tag{3.2}$$

$$\left[b_{r,\alpha/4}, b_{r,1-\alpha/4}\right] \equiv \left[\hat{y}_{r,T+h|T} - z_{\alpha/4}\sqrt{\hat{W}_{h,22}}, \quad \hat{y}_{r,T+h|T} + z_{\alpha/4}\sqrt{\hat{W}_{h,22}}\right], \tag{3.3}$$

where $z_{\alpha/4}$ is the $\alpha/4$-quantile of the standard normal distribution. Given the bivariate normality of the system (2.5), the marginal probability density functions of $y_{c,T+h}$ and $y_{r,T+h}$ are also normal.

To include the contemporaneous linear correlation between the center and log-range, we modify

the Bonferroni rectangles as in Fresoli *et al.* (2015). The corners of the modified rectangle are

$$[b_{c,\alpha/4}, \quad b_{r,\alpha/4} + p_{21,h} b_{c,\alpha/4}], \qquad [b_{c,\alpha/4}, \quad b_{r,1-\alpha/4} + p_{21,h} b_{c,\alpha/4}], \tag{3.4}$$
$$[b_{c,1-\alpha/4}, \quad b_{r,\alpha/4} + p_{21,h} b_{c,1-\alpha/4}], \qquad [b_{c,1-\alpha/4}, \quad b_{r,1-\alpha/4} + p_{21,h} b_{c,1-\alpha/4}]$$

where $p_{21,h} = \hat{W}_{h,21}/\hat{W}_{h,11}$. The area of the modified Bonferroni rectangle is the same as that of the Bonferroni rectangle. However, the theoretical coverage rate may be slightly different depending on the quantiles associated with the modified terms, e.g., $b_{r,\alpha/4} + p_{21,h} b_{c,\alpha/4}$, which in turn depend on the magnitude and sign of $p_{21,h}$. Simulations results will provide some information on the coverage rate of the modified Bonferroni rectangle. To illustrate the shapes of the three forecast regions described above, in Figure 1 we plot the 1-step-ahead 95% ellipse, Bonferroni rectangle and modified Bonferroni rectangle for the center/log-range system generated by a VAR(4) model with parameter values as reported in Table 1 and Gaussian errors with contemporaneous correlations of -0.24. The forecast regions have been obtained after estimating the parameters based on T=1000 observations so that the parameter estimation uncertainty is negligible. In Figure 1, we also plot 1000 realizations of Y_{T+1}. We observe that both the ellipse and the modified Bonferroni rectangle are able to capture the negative correlation between the center and the log-range while the Bonferroni rectangle cannot inform about this correlation. Note that the Bonferroni rectangle has large empty areas without any realization of Y_{T+1}.

3.2 Prediction regions for center/range and lower/upper systems

Moving from the center/log-range system to the center/range system or to the lower/upper bounds system, we can implement either analytical or numerical methods to construct prediction regions for the center/range system or for the lower/upper bounds system. Under bivariate normality of

center/log-range, the bivariate density of the center/range system is

$$f(y_{c,T+h}, R_{T+h}) = \frac{1}{2\pi\sqrt{|\hat{W}_h|}} \frac{1}{R_{T+h}} \exp[-\frac{1}{2}(Y_{T+h} - \hat{Y}_{T+h|T})'\hat{W}_h^{-1}(Y_{T+h} - \hat{Y}_{T+h|T})]. \tag{3.5}$$

Since the center of the interval $y_c \equiv (y_u + y_l)/2$ and the range $R \equiv (y_u - y_l)$ are linear combinations of the upper and lower bounds, it is easy to see that that the conditional bivariate density of the upper/lower bounds is also given by (3.5).

We construct analytical contours for the center/range and lower/upper bounds system by horizontally cutting the bivariate density (3.5) at a value determined by the nominal coverage $100\times(1-\alpha)\%$ that we wish to obtain. Such a value is obtained by numerical simulation. Based on the same simulated system described above, in Figure 2 we illustrate the shape of the forecast regions for the center/range system obtained using the analytical density in (3.5) by plotting the 95% forecast region and 1000 realizations of (C_{T+1}, R_{T+1}). We observe that, as expected, the region is not an ellipse. As an illustration of the shapes of the regions for the lower/upper bounds system, in Figure 3 we plot the 95% forecast regions based on (3.5) and a close-up detail of the central area of the region. In Figure 4, we plot close-ups of the extreme areas of the regions.

For the center/range system, we also construct numerical contours based on the $100 \times (1 - \alpha)\%$ normal ellipse (3.1) of the center/log-range system by transforming the points (center, log-range) sitting on the boundary of (3.1) to points (center, exp(log-range)). The new shapes will not be ellipsoids but they will maintain the coverage, and have the advantage of delivering strictly positive values for the range[3].

[3]This approach cannot be implemented to find prediction regions for the lower/upper bounds system because there is not a monotonic transformation from the boundary points of the center/log-range region to the boundary points of the lower/upper bounds region.

The $100 \times (1-\alpha)\%$ transformed normal ellipse (T-NE) is given by

$$\text{T-NE}_{T+h} = \left\{ \left[(y_{c,T+h}, \exp[\log R_{T+h}])' \right] \quad \text{such that} \quad (Y_{T+h} - \hat{Y}_{T+h|T})' \hat{W}_h^{-1} (Y_{T+h} - \hat{Y}_{T+h|T}) = q_{1-\alpha} \right\} \tag{3.6}$$

In Figure 2, we illustrate the shape of the transformed ellipse using the same simulated example previously described. The transformed shape is similar to the analytical although are not identical.

Similarly, we transform the Bonferroni and modified Bonferroni rectangles by taking the exponential transformation of the log-range intervals (3.3) and the range terms in (3.4) respectively.

Transformed Bonferroni rectangle:

$$\begin{aligned} &\left[\hat{y}_{c,T+h|T} - z_{\alpha/4} \sqrt{\hat{W}_{h,11}}, \quad \hat{y}_{c,T+h|T} + z_{\alpha/4} \sqrt{\hat{W}_{h,11}} \right] \\ &\left[\exp(\hat{y}_{r,T+h|T} - z_{\alpha/4} \sqrt{\hat{W}_{h,22}}), \quad \exp(\hat{y}_{r,T+h|T} + z_{\alpha/4} \sqrt{\hat{W}_{h,22}}) \right] \end{aligned} \tag{3.7}$$

Transformed modified Bonferroni rectangle:

$$\begin{aligned} &[b_{c,\alpha/4}, \quad \exp(b_{r,\alpha/4} + p_{21,h} b_{c,\alpha/4})], \qquad [b_{c,\alpha/4}, \quad \exp(b_{r,1-\alpha/4} + p_{21,h} b_{c,\alpha/4})], \\ &[b_{c,1-\alpha/4}, \quad \exp(b_{r,\alpha/4} + p_{21,h} b_{c,1-\alpha/4})], \quad [b_{c,1-\alpha/4}, \quad \exp(b_{r,1-\alpha/4} + p_{21,h} b_{c,1-\alpha/4})] \end{aligned} \tag{3.8}$$

In Figure 2, we illustrate the shapes of the transformed Bonferroni rectangles. Observe that while the transformed modified Bonferroni rectangle also shows the correlation between center and range, the transformed Bonferroni rectangle does not and some portions of the area are empty.

4 Non-Gaussian Center/Log-Range System

4.1 Prediction regions for the center/log-range system

Following Fresoli *et al.* (2015), we implement the following bootstrap procedure to obtain bootstrap forecasts of the center/log-range system:

Step 1. Estimate the parameters of the VAR(p) model in (2.1)-(2.2) by LS and obtain the residual vector $\hat{\varepsilon}_t = (\hat{\varepsilon}_{c,t}, \hat{\varepsilon}_{r,t})'$. Center the residuals, i.e. $\hat{\varepsilon}_t - \bar{\varepsilon}_t$ where $\bar{\varepsilon}_t = \frac{1}{T-p}\sum_{t=p+1}^{T}\hat{\varepsilon}_t$. Rescale the residuals using the factor $[\frac{T-p}{T-p-d}]^{1/2}$, where d is the number of parameters to estimate. Denote the empirical distribution of the centered and rescaled residuals as $\hat{F\varepsilon}$.

Step 2. Using the parameter estimates obtained in Step 1, generate in sample bootstrap series $\{y_{c,1}^{*(b)}, ..., y_{c,T}^{*(b)}\}$ and $\{y_{r,1}^{*(b)}, ..., y_{r,T}^{*(b)}\}$, for $t = 1, ..., T$, as follows,

$$y_{c,t}^{*(b)} = \hat{\alpha}_1 + \sum_{i=1}^{p}\hat{\beta}_{11}^{(i)} y_{c,t-i}^{*(b)} + \sum_{i=1}^{p}\hat{\beta}_{12}^{(i)} y_{r,t-i}^{*(b)} + \varepsilon_{c,t}^{*(b)}$$
$$y_{r,t}^{*(b)} = \hat{\alpha}_2 + \sum_{i=1}^{p}\hat{\beta}_{21}^{(i)} y_{c,t-i}^{*(b)} + \sum_{i=1}^{p}\hat{\beta}_{22}^{(i)} y_{r,t-i}^{*(b)} + \varepsilon_{r,t}^{*(b)},$$

where $(\varepsilon_{c,t}^{*}, \varepsilon_{r,t}^{*})'$ are random pairwise extractions with replacement from $\hat{F}_{\hat{\varepsilon}}$ and, for $t = 1, ..., p$, $y_{c,t}^{*(b)} = y_{c,t}$ and $y_{r,t}^{*(b)} = y_{r,t}$.[4]

Using $y_{c,t}^{*(b)}, y_{r,t}^{*(b)}$, estimate the VAR(p) parameters $\hat{\alpha}^{*(b)} = \begin{bmatrix} \hat{\alpha}_1^{*(b)} \\ \hat{\alpha}_2^{*(b)} \end{bmatrix}$ and $\hat{\beta}^{*(b)} = \begin{bmatrix} \hat{\beta}_{11}^{*(i)(b)} & \hat{\beta}_{12}^{*(i)(b)} \\ \hat{\beta}_{21}^{*(i)(b)} & \hat{\beta}_{22}^{*(i)(b)} \end{bmatrix}_{i=1,...,p}$.

[4] Alternatively, we can use the permutation bootstrap initially proposed by LePage and Podgorski (1996), which is expected to have a better performance in the presence of heavy-tailed errors; see Cavaliere et al. (in press) for an application to non-causal time series.

Step 3. Construct bootstrap h-step-head future values of the vector $(y_{c,T+h}, y_{r,T+h})'$ as follows,

$$\hat{y}^{*(b)}_{c,T+h|T} = \hat{\alpha}^{*(b)}_1 + \sum_{i=1}^{p} \hat{\beta}^{*(i)(b)}_{11} \hat{y}^{*(b)}_{c,T+h-i|T} + \sum_{i=1}^{p} \hat{\beta}^{*(i)(b)}_{12} \hat{y}^{*(b)}_{r,T+h-i|T} + \varepsilon^{*(b)}_{c,T+h}$$
$$\hat{y}^{*(b)}_{r,T+h|T} = \hat{\alpha}^{*(b)}_2 + \sum_{i=1}^{p} \hat{\beta}^{*(i)(b)}_{21} \hat{y}^{*(b)}_{c,T+h-i|T} + \sum_{i=1}^{p} \hat{\beta}^{*(i)(b)}_{22} \hat{y}^{*(b)}_{r,T+h-i|T} + \varepsilon^{*(b)}_{r,T+h},$$

where $\hat{y}^{*(b)}_{c,T+h-i|T} = y_{c,T+h-i}$, and $\hat{y}^{*(b)}_{r,T+h-i|T} = y_{r,T+h-i}$ for $i \geq h$, and $(\varepsilon^{*(b)}_{c,T+h}, \varepsilon^{*(b)}_{r,T+h})'$ are pairwise random draws with replacement from $\hat{F}_{\hat{\varepsilon}}$. Notice that, in order to obtain forecasts conditional on the available data set, the last p values of the original data are fixed in this step.

Step 4. Repeat steps 2 and 3 B times.

We obtain B bootstrap replicates of the vector $Y^{*(b)}_{T+h|T} = (\hat{y}^{*(b)}_{c,T+h|T}, \hat{y}^{*(b)}_{r,T+h|T})'$; see Fresoli, Ruiz, and Pascual (2015) for the asymptotic validity of the bootstrap procedure.

The bootstrap replicates obtained through the procedure proposed by Fresoli *et al.*(2015) can be used to obtain the following pointwise bootstrap ellipsoid with $100 \times (1-\alpha)\%$ coverage

$$BE_{T+h} = \left[Y_{T+h} | [Y_{T+h} - \bar{Y}^{*}_{T+h|T}]' S_{Y^*}(h)^{-1} [Y_{T+h} - \bar{Y}^{*}_{T+h|T}]\right] \leq q^{*}_{1-\alpha}, \tag{4.1}$$

where $\bar{Y}^{*}_{T+h|T}$ is the sample mean of the B bootstrap replicates $Y^{*(b)}_{T+h|T}$, $S_{Y^*}(h)$ is the corresponding sample covariance matrix and $q^{*}_{1-\alpha}$ is the $(1-\alpha)$ quantile of the empirical distribution of the quadratic form $[Y^{*(b)}_{T+h} - \bar{Y}^{*}_{T+h|T}]' S_{Y^*}(h)^{-1} [Y^{*(b)}_{T+h} - \bar{Y}^{*}_{T+h|T}]$.

Pointwise bootstrap prediction regions for the center/log-range system can also be constructed as Bonferroni rectangles with at least $100 \times (1-\alpha)\%$ coverage with the following corners

$$[q^{*}_{c,\alpha/4}, q^{*}_{r,\alpha/4}], \quad [q^{*}_{c,\alpha/4}, q^{*}_{r,1-\alpha/4}], \quad [q^{*}_{c,1-\alpha/4}, q^{*}_{r,\alpha/4}], \quad [q^{*}_{c,1-\alpha/4}, q^{*}_{r,1-\alpha/4}] \tag{4.2}$$

where $q^{*}_{c,\alpha/4}$ and $q^{*}_{r,\alpha/4}$ are the $\alpha/4$ quantiles from the respective marginal bootstrap distributions

of the center and the log-range.

If we wish to correct for the contemporaneous correlation between the center and the log-range, we construct a pointwise bootstrap modified Bonferroni rectangle with the following corners

$$[q^*_{c,\alpha/4}, q^*_{r,\alpha/4} + p^B_{21,h} q^*_{c,\alpha/4}], \quad [q^*_{c,\alpha/4}, q^*_{r,1-\alpha/4} + p^B_{21,h} q^*_{c,\alpha/4}], \tag{4.3}$$
$$[q^*_{c,1-\alpha/4}, q^*_{r,\alpha/4} + p^B_{21,h} q^*_{c,1-\alpha/4}], \quad [q^*_{c,1-\alpha/4}, q^*_{r,1-\alpha/4} + p^B_{21,h} q^*_{c,1-\alpha/4}]$$

where $p^B_{21,h} = S_{Y^*}(h)_{21}/S_{Y^*}(h)_{11}$.

Note that neither the bootstrap ellipsoid nor the Bonferroni rectangles need to be probability-centered when the joint distribution of the center/log-range system is not normal; see, for example Beran (1993) for the desirable properties of multivariate forecast regions. In this case, these regions will be only approximations to the true shape of the bootstrap forecasts. Alternatively, probability-centered forecast regions can be constructed using the convex hull peeling method of Tukey (1975); see Green (1985) for a description.[5] The Tukey peeling method consists of constructing a series of convex prediction polygons. Given a data cloud, the first layer of the Tukey convex hull is the convex polygon formed by the boundary of the data. It continues by peeling the first layer off and finding the second layer for the remaining data. This process is repeated until no convex polygon can be constructed anymore. In our case, we have a two-dimensional bootstrap data cloud $Y^{*(b)}_{T+h|T} = (\hat{y}^{*(b)}_{c,T+h|T}, \hat{y}^{*(b)}_{r,T+h|T})'$. We construct layers of convex polygons and we choose the polygon that provides the closest coverage to the desired nominal coverage rate. This is the Tukey nonparametric region. The bootstrap forecast regions for the center/log-range system can obviously be also constructed even if the errors are normal. As an illustration, Figure 1 we plot the 95% bootstrap ellipse and the Bonferroni and modified Bonferroni rectangles when the data is generated by the same data generating process described in the previous section. These regions

[5]One can also construct prediction regions using the High Density Regions proposed by Hyndman (1996) based on kernel estimates of the joint bootstrap empirical density or using the Monge-Kantorovich distance as proposed by Chernozhukov *et al.* (2017).

are based on B=4000 bootstrap replicates. Given the large sample size $T = 1000$ to estimate the parameters, the uncertainty due to parameter estimation is negligible. Consequently, the normal and bootstrap ellipses have identical shapes. The Tukey hull follows very closely the ellipses. The bootstrap Bonferroni rectangles are also very similar to their normal counterparts.

4.2 Prediction regions for center/range and lower/upper systems

As in the previous section, we can construct prediction regions for the center/range system based on the bootstrap $100 \times (1-\alpha)\%$ ellipsoid (4.1) of the center/log-range system. By transforming the points (center, log-range) sitting on the boundary of (4.1) to points (center, exp(log-range)), we obtain the $100 \times (1-\alpha)\%$ transformed bootstrap ellipse (T-BE)

$$\text{T-BE}_{T+h} = \left\{ \left[(y_{c,T+h}, \exp[\log R_{T+h}])' \right] \quad \text{such that} \quad (Y_{T+h} - \bar{Y}^*_{T+h|T})' S_{Y^*}(h)^{-1} (Y_{T+h} - \bar{Y}^*_{T+h|T}) = q^*_{1-\alpha} \right\} \tag{4.4}$$

Similarly, we obtain the transformed bootstrap Bonferroni rectangle for the center/range system with corners

$$[q^*_{c,\alpha/4}, \exp(q^*_{r,\alpha/4})], \quad [q^*_{c,\alpha/4}, \exp(q^*_{r,1-\alpha/4})], \quad [q^*_{c,1-\alpha/4}, \exp(q^*_{r,\alpha/4})], \quad [q^*_{c,1-\alpha/4}, \exp(q^*_{r,1-\alpha/4})] \tag{4.5}$$

and the transformed bootstrap modified Bonferroni rectangle with corners

$$\begin{aligned} &[q^*_{c,\alpha/4}, \exp(q^*_{r,\alpha/4} + p^B_{21,h} q^*_{c,\alpha/4})], \quad [q^*_{c,\alpha/4}, \exp(q^*_{r,1-\alpha/4} + p^B_{21,h} q^*_{c,\alpha/4})], \\ &[q^*_{c,1-\alpha/4}, \exp(q^*_{r,\alpha/4} + p^B_{21,h} q^*_{c,1-\alpha/4})], \quad [q^*_{c,1-\alpha/4}, \exp(q^*_{r,1-\alpha/4} + p^B_{21,h} q^*_{c,1-\alpha/4})] \end{aligned} \tag{4.6}$$

where $p^B_{21,h}$ is defined as in (4.3).

We also construct the Tukey nonparametric region for the data cloud of bootstrap realizations of

center and range $(\hat{y}^{*(b)}_{c,T+h|T}, \exp(\hat{y}^{*(b)}_{r,T+h|T}))'$. In Figure 2, we plot these regions for the same simulated system considered above.

Finally, for the lower/upper bounds system, we calculate first the bootstrap upper and lower bounds based on the bootstrap realizations of the center and range as follows

$$y^{*(b)}_{u,T+h} = \hat{y}^{*(b)}_{c,T+h|T} + \frac{1}{2}\exp(\hat{y}^{*(b)}_{r,T+h|T}) \tag{4.7}$$

$$y^{*(b)}_{l,T+h} = \hat{y}^{*(b)}_{c,T+h|T} - \frac{1}{2}\exp(\hat{y}^{*(b)}_{r,T+h|T}) \tag{4.8}$$

and construct a bootstrap ellipsoid for the upper and lower bounds as

$$BE^{UL}_{T+h} = \left[Y^{UL}_{T+h} | \ [Y^{UL}_{T+h} - \bar{Y}^{UL*}_{T+h|T}]' S^{UL}_{Y^*}(h)^{-1} [Y^{UL}_{T+h} - \bar{Y}^{UL*}_{T+h|T}] \leq q^{UL*}_{1-\alpha}\right] \tag{4.9}$$

where $Y^{UL}_{T+h} = (y_{u,T+h}, y_{l,T+h})'$ and $\bar{Y}^{UL*}_{T+h|T}$ and $S^{UL}_{Y^*}(h)$ represents the mean vector and variance covariance matrix, respectively, of the bootstrap upper/lower bound realizations.

Finally, a Tukey nonparametric region can be constructed for the data cloud of bootstrap realizations of upper and lower bounds $(y^{*(b)}_{u,T+h}, y^{*(b)}_{l,T+h}))'$. Note that for this system, we do not construct Bonferroni rectangles because they may contain unfeasible subregions of points where the lower bound is greater than the upper bound.

In Figures 1-4, we illustrate the shapes of the different prediction regions. We run a single simulation to construct the one-step-ahead 95%-probability forecast regions based on the estimation of a VAR(4) model ($T = 1000$) for the center/log-range system whose errors follow a bivariate normal distribution with contemporaneous correlation of -0.24. For the bootstrap procedures, we use $B = 4000$. In Figure 1, we plot seven regions for the center/log-range system. As expected, the Normal ellipse and the bootstrap ellipse have identical shapes. The Tukey convex hull follows very closely the ellipses. The modified Bonferroni rectangles are able to capture the negative correlation between center and log-range. In Figure 2, we plot the seven regions for the center/range

system. As expected, the transformed Normal ellipse and the transformed bootstrap ellipse have identical shapes. The Tukey convex hull and the analytical contour based on (3.5) follow very closely the transformed ellipses. In Figures 3 and 4, we plot the 95% bootstrap forecast ellipsoid and the Tukey region for the upper/lower bounds system. The analytical contour based on (3.5) and the Tukey convex hull are very close to each other. However, for this particular realization, the bootstrap ellipsoid is somehow different mainly in the center and upper right corner of the distribution of the lower/upper bounds system.

5 Evaluation of the Prediction Regions

We present several criteria to evaluate the prediction regions. As in the case of loss functions, it is only the objective of the forecaster that will define which criterium is the most appropriate.

At the most basic level, the forecaster will aim for reliability, that is, those prediction regions that provide the closest coverage to the nominal coverage rate. In an out-of-sample environment, for a regions with $100 \times (1-\alpha)\%$ nominal coverage, the **average coverage rate** is defined as

$$C_{(1-\alpha)} \quad = \quad \frac{1}{N} \sum_{t=1}^{N} I_t^{(1-\alpha)} \tag{5.1}$$

where N is the number of out-of-sample forecasts and $I_t^{(1-\alpha)}$ is an indicator variable that is equal to 1 if the observed outcome falls within the prediction region and 0 otherwise.

Following Golestaneh *et al.* (2017), we combine reliability with sharpness, a preference for regions with smaller area or volume, and they propose the following **average coverage-volume score** for regions with $100 \times (1-\alpha)\%$ nominal coverage

$$CV_{(1-\alpha)} \quad = \quad \Big| \frac{1}{N} \sum_{t=1}^{N} \big[I_t^{(1-\alpha)} - (1-\alpha) \big] \times \big[V_t^{(1-\alpha)} \big]^{\frac{1}{p}} \Big| \tag{5.2}$$

where $V_t^{(1-\alpha)}$ is the volume of the prediction region with nominal coverage rate $(1-\alpha)$ at time t, and p is the dimension of the outcome variable, which in our case is $p = 2$. The forecaster would prefer a lower score as he is aiming for regions with high reliability and small area.

Another aspect to the evaluation of forecast regions is to consider the observations outside of the $100 \times (1-\alpha)\%$ region and to assess how far they are from a central point within the prediction region. We propose the following **average outlier distance**

$$O_{(1-\alpha)} = \frac{1}{G} \sum_{t=1}^{N} \left[1 - I_t^{(1-\alpha)}\right] \times D(y_t, M_t) \tag{5.3}$$

where G is the number of observations outside the region, D is a distance measure (e.g. Euclidean distance) of each outside-the-region outcome y_t from M_t, which is a central point in the region. We choose M_t to be the median of the realizations generated at each time t according to the methods explained in Section 4. However, defining the median for a multi-dimensional dataset (2-dimensional in our case) is not as straighforward as it is for a one-dimensional dataset. To obtain M_t, we implement the definition of median in a multi-dimensional setting introduced by Zuo (2003), known as 'projection depth median', and programmed in the Matlab package (Liu and Zuo, 2015). A brief description follows.

With a one-dimensional dataset, $Z = \{Z_i\}$, $i = 1, ...n$, a robust measurement of the outlyingness of a point z (a scalar) relative to Z is the outlying function

$$o_1(z, Z) = \frac{|z - Med(Z)|}{MAD(Z)}$$

where Med is the median of data set Z and $MAD(Z) = Med\{|Z_i - Med(Z)|, i = 1, ..., n\}$. When z and Z are p-dimensional ($p > 1$), the above outlying function is applied by projecting z and Z into a one-dimensional space, i.e., $o_1(u^T z, u^T Z)$, where $u \in S$ and $S = \{v \in R^p : \|v\| = 1\}$ is a set of unit vectors in the p-dimensional space. The projection depth of point z with respect to Z

is defined as $PD(z, Z) = (1 + O(z, Z))^{-1}$, where $O(z, Z) \equiv \sup_{u \in S} o_1(u^T z, u^T Z)$. Under some mild conditions (Zuo, 2013), there exists a unique single point ($z^* \in R^p$, not necessarily from Z) that maximizes $PD(z, Z)$ for a data set Z. This z^* is defined as the 'projection depth median' of Z.

The $100 \times \alpha\%$ outside-the-region observations can be considered 'risk' that the forecaster has to bear and, in this sense, he would like to minimize $O_{(1-\alpha)}$. For two regions with similar coverage, the forecaster will choose that with a lower average outlier dispersion.

We also evaluate the prediction region by the sharpness or tightness of the intervals that result from projecting the two-dimensional region into one-dimensional intervals. We draw a large number of directions, which are given by the lines drawn from the zero origin of the unit circle to any point in its boundary. For each direction, we find the two bounding tangent lines to the prediction region that are perpendicular to that direction. We calculate the length of the projected interval bounded by the tangent lines. See Figure 5 (top panel) for a graphical representation. Denote $d_i \in \Upsilon$ as the i^{th} direction in Υ, where Υ is the set of all directions, and let D be the number of directions. At time t, the average projection length over all directions is

$$P_t = \frac{1}{D} \sum_{i=1}^{D} (u_{d_i} - l_{d_i}),$$

where u_{d_i} is the upper bound and l_{d_i} the lower bound of the projected interval in the i^{th} direction. Then, over the prediction sample, the **average length of the projected intervals** associated with the $(1 - \alpha)\%$ prediction region is

$$P_{(1-\alpha)} = \frac{1}{N} \sum_{t=1}^{N} P_t \tag{5.4}$$

The forecaster would prefer prediction regions that deliver tight projected intervals.

We now consider the realized data points over the prediction period in conjunction with the projected intervals. For each direction, we also project each point into that direction and measure

whether the point falls into or outside of the projected interval (see Figure 5, top panel) . An indicator function I will assign the value 0 if the point falls inside and 1 if the point falls outside of the projected interval. At time t, over all D directions, we calculate the average distance of the projected outliers to the projected interval as

$$OP_t = \frac{1}{D}\sum_{i=1}^{D}[(l_{d_i} - x_{d_i})I(x_{d_i} < l_{d_i}) + (x_{d_i} - u_{d_i})I(x_{d_i} > u_{d_i})]$$

where x_{d_i} is the coordinate of the data point projected on the i^{th} direction. Then, over the prediction sample, the **average distance of the projected outliers** associated with the $100 \times (1-\alpha)\%$ prediction region is

$$OP_{(1-\alpha)} = \frac{1}{N}\sum_{t=1}^{N} OP_t \tag{5.5}$$

The forecaster prefers prediction regions with projected outliers close to the projected intervals.

We expect that when the length of the projected interval is large, the distance of the projected outliers to the interval will be smaller. To take into account this a trade-off, we propose a combined criterium $POP_t = P_t \times OP_t$ so that, over the prediction sample, the average trade-off associated with the $100 \times (1-\alpha)\%$ prediction region is

$$POP_{(1-\alpha)} = \frac{1}{N}\sum_{t=1}^{N} POP_t \tag{5.6}$$

A smaller $POP_{(1-\alpha)}$ would be preferred by the forecaster.

Finally, we assess whether the prediction region is probability-centered. We check whether the points outside of the prediction region are evenly distributed around the region. At time t, we consider a cloud of data points and calculate the median M_t as in Zuo (2003). We also consider a number of directions D that pass through M_t. We define $H_u(d_i, M_t)$ as the half-plane above the

line generated by the direction d_i and $H_l(d_i, M_t)$ as the half-plane below the same line. See Figure 5 (bottom panel) for a graphical representation. For a given direction d_i and the $100 \times (1-\alpha)\%$ prediction region R, we consider the number of points outside of the region, i.e., $x \in R^c$, which are either in $H_u(d_i, M_t)$ or in $H_l(d_i, M_t)$, that is

$$C_u(d_i, M_t)) = \{\#x | (x \in R^c) \cap (x \in H_u(d_i, M_t))\}$$
$$C_l(d_i, M_t) = \{\#x | (x \in R^c) \cap (x \in H_l(d_i, M_t))\}$$

where $C_u(d_i)$ and $C_l(d_i)$ are functions providing the number of of outlier points falling in the upper half-plane or lower half-plane respectively. If the outliers are evenly distributed around the $100 \times (1-\alpha)\%$ prediction region, we expect the following statistic $S_{(1-\alpha)}(M_t)$ to be close to zero

$$S_{(1-\alpha)}(M_t) = \frac{1}{D} \sum_{i=1}^{D} |C_u(d_i, M_t)) - C_l(d_i, M_t)| \tag{5.7}$$

Though $S_{(1-\alpha)}(M_t)$ will not be feasible with real data (we will have only one realized observation at time t that could be in or out of the prediction region), in a simulated environment, we will be able to assess the probability-centered property of each prediction region.

6 Monte Carlo Simulations

We perform extensive Monte Carlo simulations to assess the performance of the prediction regions constructed with the analytical and semiparametric methods explained in sections 3 and 4. The regions are evaluated according to the seven criteria described in section 5.

We generate a small sample of $T = 200$ observations and a large sample of $T = 1000$ observations (estimation samples) from a VAR(4) for the center/log-range system (2.1)-(2.2) with parameter values reported in Table 1. We consider four cases regarding distributional assumptions from which

the errors are drawn: (1) center and log-range errors are both normally distributed; (2) center errors are Student-t with 5 degrees of freedom and log-range errors are normally distributed; (3) center errors are Student-t with 5 degrees of freedom and range errors are exponentially (λ) distributed; and (4) center errors are normal and range errors exponentially (λ) distributed. Note that the distributional assumptions are on the marginal densities of the errors of each equation. It is only in case (1) that the bivariate density of the center and log-range is normal; in the rest of the cases, we do not know the exact bivariate densities.[6]

We consider 1- and 3-step-ahead prediction regions with 95% nominal coverage.[7] We calculate the empirical coverage by simulating 1000 future values of the required vector at time T, i.e. center/log-range, center/range, and upper/lower bounds, at the forecast horizon, and calculating the proportion of these values that falls within the constructed prediction regions. The number of Monte Carlo replications is 500, the number of bootstrap samples is $B = 2000$, and the number of directions to calculate the average length of the projected intervals and outliers is $D = 100$.

6.1 Center and Log-Range are Normally distributed

The errors of the center equation of the VAR(4) are drawn from a normal density as well as the errors of the log-range equation. In Tables 2-3, we report the evaluation of the prediction regions for the three systems (center/log-range, center/range and upper/lower bounds) for forecast horizon $h = 1$ with estimation samples $T = 1000$ and $T = 200$. Note that we only estimate the VAR(4) once for the center/log-range, construct prediction regions for this system, and based on these estimates, we proceed to construct prediction regions for the other two systems.

Given the bivariate normality of the center/log-range system, the prediction regions based on the

[6]For the system to have the desired marginal density functions and the stated correlation structure, we have generated bivariate errors from a Gaussian copula and re-transform the PITs of the corresponding univariate normal variates according to the desired density, e.g. Student-t, to obtain the new error variates, which need to be adjusted to have the desired mean and variance.

[7]The results for $h = 3$ are provided in the Supplementary Material, Tables S1-S4.

normal ellipse (3.1) and on the analytical methods (3.5) would be exact if parameter estimation were not a concern. For a large estimation sample $T = 1000$ (Table 2), all regions, except for the Tukey convex hull, are very reliable with empirical coverage C_{95} of mostly 95%. Bootstrap ellipse and bootstrap Bonferroni rectangles, which account for parameter uncertainty, deliver the closest value to 95% in the three systems. Bonferroni rectangles have the largest areas compared to the normal ellipse and to the regions based on analytical methods, but because they provide good coverage, they enjoy one of the lowest average coverage-volume scores CV_{95}. The larger area of the Bonferroni rectangles is somehow compensated by a lower average outlier distance O_{95}, though this metric is very similar for all prediction regions considered across the three systems. The tightest regions i.e., those projecting tight one-dimensional intervals measured by POP_{95}, correspond to the normal ellipse, bootstrap ellipsoids, and those regions based on exact analytical expressions. These are also the regions with outliers more evenly distributed around their boundaries.

For small estimation sample $T = 200$ (Table 3), the bootstrap regions provide a clear advantage with respect to the other regions. In small samples, parameter uncertainty plays a more important role than in large samples. Boostrap methods are designed to take into account estimation uncertainty. Across systems, bootstrap ellipsoids and bootstrap Bonferroni rectangles are still very reliable with empirical coverage close to 95%. They also enjoy the smallest score CV_{95}. The tightest regions, i.e small POP_{95}, are provided by the bootstrap ellipsoid and its transformed regions followed by the Tukey region.

Considering the overall performance assessed by the metrics C, CV, and POP, for large estimation samples, normal ellipses, bootstrap ellipsoids, and those regions based on analytical methods are the best performers, and as expected, better than the Tukey convex hull. Bonferroni rectangles, though providing good coverage, tend to be conservative in area, which in turn provides some advantages regarding the lower dispersion of the outliers. For small samples, the bootstrap ellipsoid is the best performer. These conclusions hold regardless of whether $h = 1$ or $h = 3$.

6.2 Student-t(5) Center and Normal Log-Range

In Tables 4-5, we report the performance of the different predictions regions when the errors of the center equation of the VAR(4) are leptokurtic and the errors of the log-range equation are normal. Thus, the bivariate system center/log-range is not normally distributed but symmetric. Consequently, the normal ellipse, Bonferroni rectangles, and their corresponding transformed regions tend to undercover with empirical coverage rates of about 94% in large samples, and about 93% in small samples because they do not consider the fat tails of the errors in the center equation. The bootstrap regions, which are robust to distributional assumptions and capture estimation uncertainty, are better performers with coverage rates close to 95% in large and small samples. They also provide the smallest score CV_{95} and, according to S_{95}, tend to have a more evenly distribution of outliers around the regions. For small samples, the performance of bootstrap regions is even more striking with the bootstrap ellipsoid being the best region in terms of C_{95}, CV_{95}, and S_{95}.These results hold for both horizons $h = 1$ or $h = 3$.

The Tukey regions, which do not require any distributional assumption, are in-between the bootstrap regions and the regions based on normality. Note that the Tukey regions have a superior advantage according to POP_{95}. Sacrificing a bit of coverage, the Tukey region provides the tightest one-dimensional projections across systems, estimation samples, and forecast horizons.

6.3 Student-t(5) Center and Exponential Range

In Tables 6-7, we report the performance of the different predicitons regions when the errors of the center equation of the VAR(4) are drawn from a Student-t with 5 degrees of freedom and the errors of the log-range equation are those resulting from assuming that the *range* itself is exponentially distributed. The exponential errors introduce some asymmetry that is not fully corrected when they are transformed into errors of the log-range equation. The resulting bivariate

system center/log-range is not normally distributed as it exhibits leptokurtosis and asymmetry.

For small and large samples, the bootstrap regions (ellipsoids and Bonferroni rectangles) provide the best coverage C_{95} with empirical rates very close to 95%, followed by the Tukey region that covers around 94% of the events. The same regions have the smallest scores CV_{95} and the smallest POP_{95}. As in the previous case, the Tukey region has a clear advantage over the other regions when we are interested in the smallest POP_{95}. It is interesting to note that the boostrap Bonferroni rectangles are able to distribute outliers more evenly around their perimeters than any other prediction regions. These results hold for the two horizons considered $h = 1$ and $h = 3$.

6.4 Normal Center and Exponential Range

In Tables 8-9, we report the performance of the different predictions regions when the errors of the center equation of the VAR(4) are drawn from a normal distribution and the errors of the log-range equation are those resulting from assuming that the *range* itself is exponentially distributed. The resulting bivariate system center/log-range is not normally distributed as asymmetry is introduced through the log-range equation.

For large samples, all regions have an empirical coverage C_{95} between 94 and 95% with the bootstrap ellipoid and the bootstrap Bonferroni rectangle being very close to 95%. It is interesting to note that the normal ellipse in the center/log-range system and its analytically derived regions for the center/range and upper/lower systems provide a very competitive coverage of almost 95% and the smallest scores CV_{95}. The bootstrap ellipsoid and its transformed regions come as the next best performer with some advantage regarding the POP_{95} criterium. In small samples, the boostrap methods provide the best coverage with an empirical rate of almost 95%. The bootstrap ellipsoid delivers the best performance when considering CV_{95} and POP_{95}. The normal ellipse and its analytically derived formulas tend to undercover with rates around 93%. We obtain similar results for $h = 1$ and $h = 3$.

In summary, considering the three systems (center/log-range, center/range, and upper/lower) and assessing the overall performance of the prediction regions by the summary metrics C_{95}, CV_{95}, and POP_{95}, we conclude the following:

1. If the center/log-range system is bivariate normal (case 6.1) or approximately normal (case 6.4) and the estimation sample is large, the prediction regions based on the normal ellipse (3.1) and on the analytical methods (3.5) are the best performers. However, with a small estimation sample, we recommend implementing a bootstrap ellipsoid (4.1) and its transformed regions (4.4), and (4.9).

2. If the center/log-range system is not bivariate normal but the joint distribution is symmetric (case 6.2) and the estimation sample is large, any of the bootstrap regions (ellipsoids and Bonferroni rectangles) (4.1, (4.2), and (4.3), their transformed (4.4), (4.5), (4.6), as well as (4.9) are the best performers. In small samples, a bootstrap ellipsoid (4.1) and its transformed regions (4.4), as well as (4.9) are preferred.

3. If the center/log-range system is not bivariate normal and the joint distribution is leptokurtic and asymmetric (case 6.3), for large and small samples, we recommend implementing the bootstrap Bonferroni rectangles (4.2), and (4.3) and their transformed (4.5), (4.6), as well as (4.9).

7 Prediction Regions for SP500 Low/High Return Interval

We collect the daily intervals of low/high prices of the SP500 index from January 2, 2009 to April 20, 2018 for a total of 2341 observations. Since prices are non-stationary, we construct the daily interval of low/high returns by calculating the daily minimum and maximum returns with respect to the closing price of the previous day. In this way, we will model stationary intervals. In the Supplementary Material Table S5, we provide the descriptive statistics of the center, range and log-range of the low/high return intervals. The center average is zero with a standard deviation of 0.64. The center exhibits fat tails with a coefficient of kurtosis of 7 and it is slightly skewed to

the left. The range has a mean of 1.15 and a larger standard deviation, 0.83, than the center, it is positively skewed, and it is negatively correlated with the center with a coefficient of correlation of -0.12. The log-transformation of the range corrects the asymmetry and large kurtosis of the range so that log-range is only slightly skewed to the right and has a coefficient of kurtosis of about 3. The coefficient of correlation of center and log-range is about -0.10. The Q-statistics for the center indicate no autocorrelation while those for the range and log-range indicate high autocorrelation. In Figure 6, we plot the time series of the center and the range as well as their unconditional bivariate density function. The heavy tails in the center and the almost normality of the log-range are similar distributional characteristics to those of the simulation case in section 6.2 (Student-t(5) center and normal log-range).

We proceed with the modeling of the bivariate system of center/log-range. We split the total sample into an estimation sample from January 2, 2009 to December 31, 2016 (2014 observations) and a prediction/evaluation sample from January 1, 2017 to April 20, 2018 (327 observations). The autocorrelograms of the center seem to indicate no autocorrelation in contrast to those of the log-range that exhibit a profile of an AR(6) with strong memory (see Figure S1 in the Supplementary Material). These features mimic the autocorrelation that we observe in the end-of-the day returns and in their squared returns when modeling the conditional variance, which is not very surprising because range or log-range are good proxies for volatility. The SIC also selects a VAR(6) and we proceed with the VAR estimation. The results are presented in Table S6 of the Supplementary Material. As expected, all the regressors (lagged center and lagged log-range) in the equation for the center are not statistically significant and we re-estimate a restricted VAR where the center equation has only a constant. On the contrary, the equation for the log-range present interesting dynamics. The center Granger-causes the log-range such that the lagged centers are negatively correlated with the current log-range, i.e. positive and large changes in the center return today will predict a narrower range tomorrow. This is similar to a leverage effect in a conditional variance equation. Another relevant aspect is the strong and statistically significant autoregressive nature of

log-range in agreement with the ACF/PACF profiles. The goodness of fit for the log-range equation is high with an adjusted R-squared of 52%. The residuals corresponding to this system are all clear of any autocorrelation. The center residuals and log-range residuals are contemporaneous negatively correlated with a correlation coefficient of -0.17. The residuals from the center equation have the same characteristics as the center, that is, are leptukortic with a sample kurtosis of 7 and slightly skewed to the left. The residuals from the log-range equation remain almost symmetric around zero and they have a sample kurtosis of 3. With these characteristics, the conditional joint density of the center and log-range cannot be bivariate normal.

Formally, we test for conditional bivariate normality by implementing the Generalized AutoContouR (G-ACR) (in-sample) tests based on the Probability Integral Transformations (PIT) of the joint density under the null hypothesis of bivariate normality (González-Rivera and Sun, 2015). In Table S7 of the Supplementary Material, we report the results of the t-statistics ($t_{k,\alpha}$) that canvas the density from the 1% to the 99% PIT autocontours for lags $k = 1, 2, ...5$. The null hypothesis is strongly rejected at the 5% significance level for mostly all but the 10%, 90% and 95% autocontours. The portmanteau test C_k also reinforces the strong rejection of bivariate normality. In Figure S2 of the Supplementary Material, we plot the autocontours of the contemporaneous PITs $(\text{center}_t, \text{log-range}_t|\text{center}_t)$. Under the correct null hypothesis, the distribution of the PITs should be uniformly distributed within these autocontour squares. It is obvious that this is not the case.

We evaluate the out-of-sample performance of the one-step-ahead 95% prediction regions from January 1, 2017 to April 20, 2018 (327 observations). The results are reported in Tables 10. For the system center/log-range, the bootstrap Bonferroni rectangles (4.2) and (4.3) offer the best coverage C_{95} with empirical rates of mostly 95% and they are the most reliable with the lowest average coverage-volume scores CV_{95}. Together with the Tukey convex hull, they also provide the lowest average outlier distance O_{95}. Both rectangles (4.2) and (4.3) also provide the tightest projected one-dimensional regions measured by POP_{95}. For the system center/range, we find that

the transformed modified bootstrap Bonferroni rectangle (4.6) is the best performer according to most metrics C_{95}, CV_{95} and POP_{95}. For the system upper/lower bounds, the Tukey convex hull offers the best coverage and the lowest scores for O_{95} and POP_{95}. As expected, the analytic methods (3.5) are not reliable as they tend to undercover. On the contrary, the bootstrap ellipsoid (4.1) and its transformed region (4.4), and (4.9) tend to overcover. All these results are very consistent with the Monte Carlo findings of the previous section.

In Figures 7 and 8, we plot the one-step ahead 95% prediction regions for the center/log-range and center/range systems respectively. We choose six random dates over the prediction sample (March 15, May 11, August 30, December 8, 2017 and February 22, April 6, 2018). In all six dates, the one-step-ahead realized values of the (center, log-range) and (center, range) fall within the regions; only the realized values on December 8, 2017 and April 6, 2018 are slightly more extreme and they fall towards the boundaries of the prediction regions. For the center/log-range system, the normal ellipse and the bootstrap ellipse are very similar but in the center/range system, the bootstrap ellipse tends to be wider adapting to the kurtosis of the center and the asymmetry of the range. The differences among the Bonferroni rectangles are more obvious in the center/range system. In the center/log-range system, the Tukey convex hull has a cone shape over all the six dates though the shape becomes more irregular in the center/range system.

8 Conclusion

The interest in interval data arises because interval measurements offer a more complete description of a data set. In time series, each time realization has joint information on the level and the dispersion of the process under study. However, statistical analysis of interval-valued data requires that the natural order of the interval is preserved. Though there are several works that consider the problem of estimation with constraints, we are not aware of any work that considers the

construction of forecasts for interval-valued data satisfying the natural constraint in each period of time, i.e. lower bound is not larger than the upper bound, or equivalently, the range of the interval must be strictly positive. Our contribution lies on approximating a probabilistic forecast of an interval-valued time series by offering alternative approaches to construct bivariate prediction regions of the center and the range, or the lower and upper bounds, of the interval.

To overcome the positive constraint of the range, we have estimated a Gaussian bivariate system for the center/log-range system, which also delivers QML properties for our estimators. However, the interest of the researcher is not the prediction of the center/log-range but the center/range or upper/lower bounds of the interval. By implementing either analytical or bootstrap methods we have directly transformed the prediction regions for the center/log-range system into those for the center/range and upper/lower bounds systems. It is important to remark that we do not focus on point forecast purposely. By focusing on prediction regions rather than on point forecasts, we avoid the biases that are associated with the exp-transformation of the point forecasts of log-transformed variable. In this case, bias-correction techniques are necessary if one's interest is the conditional mean of the future variable. A prediction region for the center/log-range does not need any bias correction when we transform it to a prediction region of the center/range system because the quantile is preserved under a monotonic transformation like the exp-transformation. However, these transformed prediction regions can have very irregular shapes even in the most straightforward scenario of bivariate normality of the center/log-range system. If a central point forecast is of interest, the researcher can always calculate the centroid of the region.

Beyond the standard coverage rate, we have proposed several new metrics to evaluate the performance of different prediction regions. We have introduced a notion of risk to the evaluation of the regions by considering the location of the out-of-the-region outcomes with respect to some central point in the region. The researcher would like to minimize risk once the empirical coverage of the region is close to the nominal coverage. We have considered Gaussian and non-Gaussian systems

and our recommendation leans towards bootstrap methods, even for Gaussian systems. Bootstrap ellipsoids and their transformed are best when the joint distribution of the center/log-range system is symmetric. If it is not, then bootstrap Bonferroni rectangles will be preferred.

We have analyzed the time series of the daily low/high return interval of the SP500 index. We modeled and predicted the *joint* conditional density of the return level and the return volatility. We showed that the construction of several prediction regions of the center and range of the return interval do not require strong parametric distributional assumptions.

References

[1] Alizadeh, S., M. W. Brandt, & F.X. Diebold (2002). Range-based Estimation of Stochastic Volatility Models. *Journal of Finance*, 57(3), pp. 1047-1091.

[2] Ariño, M.A., & P. Franses (2000). Forecasting Levels of Vector Autoregressions Log-transformed Time Series. *International Journal of Forecasting*, 16, pp. 111-116.

[3] Bardsen, G., & H. Lutkepohl (2011). Forecasting Levels of Log Variables in Vector Autoregressions. *International Journal of Forecasting*, 27, pp. 1108-1115.

[4] Beran, R. (1993). Probability-Centered Prediction Regions. *Annals of Statistics*, 21(4), pp. 1967-1981.

[5] Blanco-Fernádez, A. & P. Winker (2016). Data Generation and Statistical Management of Interval Data. *AStA Advances in Statistical Analysis*, 10(4), pp. 475-494.

[6] Cavaliere, G., H.B. Nielsen & A. Rahbek (in press). Bootstrapping Non-causal Autoregressions with Applications to Explosive Bubble Modeling. *Journal of Business & Economic Statistics*.

[7] Chernozhukov V., A. Galichon, M. Hallin & M. Henry (2017). Monge-Lontorovich Depth, Quantiles, Ranks and Signs.*Annals of Statistics*, 45(1), pp. 223-256.

[8] Fresoli, D., E. Ruiz, & L. Pascual (2015). Bootstrap Multi-step Forecasts for Non-Gaussian VAR Models. *International Journal of Forecasting*, 31, pp. 834-848.

[9] Golestaneh, F., P. Pinson, R. Azizipanah-Abarghooee, & H.B. Gooi (2018). Ellipsoidal Prediction Regions for Multivariate Uncertainty Characterization. *IEEE Transactions on Power Systems*, 33(4), pp. 4519-4530.

[10] González-Rivera, G., & W. Lin (2013). Constrained Regression for Interval-valued Data. *Journal of Business and Economic Statistics*, 31(4), pp. 473–490.

[11] González-Rivera, G., & Y. Sun (2015). Generalized Autocontours: Evaluation of Multivariate Density Models. *International Journal of Forecasting*, 31(3), pp. 799-814.

[12] ranger, C.W.J. & P. Newbold (1976). Forecasting Transformed Series. *Journal of the Royal Statistical Society, B*, 38, pp. 189-203.

[13] Green, W. (1985). Peeling Data. *Encyclopedia of Statistical Sciences*, 6, pp. 660-664.

[14] Guerrero, V.M. (1993). Time Series Analysis Supported by Power Transformation. *Journal of Forecasting*, 12, pp. 37-48.

[15] Hyndman, R.J. (1996). Computing and Graphing Highest Density Regions. *The American Statistician*, 50, pp. 120-126.

[16] LePage, R. & K. Podgorski (1996). Resampling Permutations in Regressions without a Second Moment. *Journal of Multivariate Analysis*, 57, pp. 119-141.

[17] Lima Neto, E., & F. de Carvalho (2010). Constrained Linear Regression Models for Symbolic Interval-Valued Variables. *Computational Statistics and Data Analysis*, 54, pp. 333-347.

[18] Liu, X. & Y. Zuo (2015). CompPD: A MATLAB Package for Computing Projection Depth. *Journal of Statistical Software*, 65(2).

[19] Lutkephol, H. (1991). *Introduction to Multiple Time Series Analysis*, Springer-Verlag, Berlin.

[20] Mayr, J., & D. Ulbricht (2015). Log versus Level in VAR Forecasting: 42 Million Empirical Answers. Expect the Unexpected. *Economics Letters*, 126, pp. 40-42.

[21] Parkinson, M. (1980). The Extreme Value Method for Estimating the Variance of the Rate of Return. *Journal of Business*, 53(1), pp. 61-65.

[22] Pascual L., J. Romo & E. Ruiz (2005). Bootstrap Prediction Intervals for Power Transformed Time Series. *International Journal of Forecasting*, 21, pp. 219-235.

[23] Tu, Y., & Y. Wang (2016). Center and Log Range Models for Interval-valued Data with An Application to Forecast Stock Returns. Working paper.

[24] Tukey, J. (1975). Mathematics and Picturing Data, in *Proceedings of the 1975 International Congress of Mathematics*, 2, pp. 523-531.

[25] White, H. (1982). Maximum Likelihood Estimation of Misspecified Models. *Econometrics*, 50, pp.1-25.

[26] Yao, W., & Z. Zhao (2013). Kernel Density-based Linear Regression Estimate. *Communications in Statistics. Theory and Methods*, 42(24), pp. 4499-4512.

[27] Zuo, Y. (2003). Projection-based Depth Functions and Associated Medians. *Annals of Statistics*, 31(5), pp. 1460-1490.

[28] Zuo Y. (2013). Multidimensional Medians and Uniqueness. *Computational Statistics & Data Analysis*, 66, pp. 82-88

Tables: Monte Carlo Simulations.

	Center equation	log-Range equation
Constant	-0.9344	0.0759
C(-1)	0.3404	-0.0112
C(-2)	-0.1530	-0.0027
C(-3)	0.0314	-0.0030
C(-4)	-0.0551	-0.0022
log-R(-1)	-0.5030	0.0852
log-R(-2)	0.1281	0.1845
log-R(-3)	-0.1556	0.1539
log-R(-4)	0.9157	0.0760

Variance-covariance matrix of the errors:

$$\Omega = \begin{bmatrix} \sigma_1^2 & \sigma_{12} \\ \sigma_{12} & \sigma_2^2 \end{bmatrix} = \begin{bmatrix} 111.24 & -1.02 \\ -1.02 & 0.16 \end{bmatrix}$$

Contemporaneous correlation between the center and log-range errors = -0.24.

Table 1: Monte Carlo simulations. VAR(4) parameter values for the center/log-range system

Large Estimation Sample $T = 1000$	EVALUATION CRITERIA							
CENTER/log-RANGE system	C_{95}	$V^{1/2}$	CV_{95}	O_{95}	P_{95}	OP_{95}	POP_{95}	S_{95}
NE: Normal ellipse (3.1)	0.9469	8.7059	0.0645	18.8891	25.8596	0.0275	0.7090	0.0089
Bonferroni rectangle (3.2)-(3.3)	0.9484	9.1321	0.0646	18.3628	24.9220	0.0375	0.9309	0.0088
Modified Bonferroni rectangle (3.4)	0.9516	9.1321	0.0655	18.5670	24.9306	0.0372	0.9255	0.0095
BE: Bootstrap ellipsoid (4.1)	0.9493	8.7842	0.0801	19.0161	26.0994	0.0262	0.6773	0.0087
Bootstrap Bonferroni rectangle (4.2)	0.9493	9.2184	0.0819	18.4758	25.1222	0.0373	0.9293	0.0096
Modified Bootstrap Bonferroni rectangle (4.3)	0.9521	9.2184	0.0848	18.6347	25.1309	0.0371	0.9240	0.0104
Tukey convex hull	0.9414	8.6389	0.1028	18.5770	26.1263	0.0283	0.7265	0.0107

CENTER/RANGE system	C_{95}	$V^{1/2}$	CV_{95}	O_{95}	P_{95}	OP_{95}	POP_{95}	S_{95}
Analytical method (3.5)	0.9470	9.8933	0.0782	18.7056	26.2543	0.0263	0.6885	0.0161
T-NE: T-Normal ellipse (3.6)	0.9469	10.1606	0.0756	18.9612	25.9781	0.0280	0.7259	0.0089
T-Bonferroni rectangle (3.7)	0.9484	10.7382	0.0758	18.4471	25.4849	0.0349	0.8849	0.0088
T-Modified Bonferroni rectangle (3.8)	0.9513	10.9309	0.0788	18.5675	25.5757	0.0343	0.8742	0.0101
T-BE: T-Bootstrap ellipsoid (4.4)	0.9493	10.2637	0.0940	19.0892	28.8440	0.0267	0.7346	0.0087
T-Bootstrap Bonferroni rectangle (4.5)	0.9493	10.8482	0.0966	18.5638	25.6943	0.0347	0.8832	0.0096
T-Modified Bootstrap Bonferroni rectangle (4.6)	0.9519	11.0436	0.1036	18.6581	25.7867	0.0342	0.8722	0.0109
Tukey convex hull	0.9411	10.2071	0.1237	18.6050	26.2517	0.0287	0.7406	0.0119

UPPER/LOWER system	C_{95}	$V^{1/2}$	CV_{95}	O_{95}	P_{95}	OP_{95}	POP_{95}	S_{95}
Analytical method (3.5)	0.9470	9.8763	0.0781	26.3045	46.5574	0.0463	2.1514	0.0095
Bootstrap ellipsoid (4.9)	0.9488	10.4679	0.1010	24.3205	47.3650	0.0414	1.9393	0.0126
Tukey convex hull	0.9411	10.1884	0.1232	26.1956	46.5761	0.0506	2.3167	0.0114

Table 2: Evaluation of the h-step ahead 95% prediction regions from a **GAUSSIAN center/log-range system** ($h = 1$); 500 Monte Carlo simulations from a VAR(4). In the first column, the numbers in parenthesis e.g., (x.x) are the corresponding equations in the text.

Small Estimation Sample $T = 200$	EVALUATION CRITERIA							
CENTER/log-RANGE system	C_{95}	$V^{1/2}$	CV_{95}	O_{95}	P_{95}	OP_{95}	POP_{95}	S_{95}
NE: Normal ellipse (3.1)	0.9323	8.5326	0.1687	18.4343	25.4321	0.0369	0.9220	0.0208
Bonferroni rectangle (3.2)-(3.3)	0.9352	8.9625	0.1559	18.0943	24.5124	0.0490	1.1831	0.0198
Modified Bonferroni rectangle (3.4)	0.9378	8.9625	0.1421	18.1143	24.5209	0.0488	1.1768	0.0201
BE: Bootstrap ellipsoid (4.1)	0.9465	8.9272	0.1302	19.0901	26.6052	0.0276	0.7146	0.0172
Bootstrap Bonferroni rectangle (4.2)	0.9455	9.3834	0.1384	18.4711	25.6546	0.0408	1.0206	0.0181
Modified Bootstrap Bonferroni rectangle (4.3)	0.9480	9.3834	0.1320	18.4979	25.6636	0.0406	1.0152	0.0178
Tukey convex hull	0.9334	8.7457	0.1775	18.3070	26.8745	0.0310	0.8045	0.0222

CENTER/RANGE system	C_{95}	$V^{1/2}$	CV_{95}	O_{95}	P_{95}	OP_{95}	POP_{95}	S_{95}
Analytical method (3.5)	0.9327	9.7378	0.1927	18.4312	25.8139	0.0356	0.9029	0.0247
T-NE: T-Normal ellipse (3.6)	0.9323	9.9933	0.1971	18.5044	25.5514	0.0376	0.9434	0.0209
T-Bonferroni rectangle (3.7)	0.9352	10.5726	0.1836	18.1739	25.0743	0.0457	1.1273	0.0199
T-Modified Bonferroni rectangle (3.8)	0.9373	10.7899	0.1750	18.1043	25.1757	0.0450	1.1140	0.0208
T-BE: T-Bootstrap ellipsoid (4.4)	0.9465	10.4975	0.1528	19.1640	26.7346	0.0281	0.7324	0.0173
T-Bootstrap Bonferroni rectangle (4.5)	0.9455	11.1567	0.1645	18.5525	26.2772	0.0378	0.9673	0.0181
T-Modified Bootstrap Bonferroni rectangle (4.6)	0.9472	11.3987	0.1633	18.4061	26.3916	0.0371	0.9548	0.0187
Tukey convex hull	0.9338	10.4532	0.2114	18.3920	27.0735	0.0311	0.8151	0.0224

UPPER/LOWER system	C_{95}	$V^{1/2}$	CV_{95}	O_{95}	P_{95}	OP_{95}	POP_{95}	S_{95}
Analytical method (3.5)	0.9327	9.7528	0.1931	25.9290	45.7581	0.0629	2.8261	0.0198
Bootstrap ellipsoid (4.9)	0.9470	10.7473	0.1919	25.1246	48.4270	0.0429	2.0190	0.0180
Tukey convex hull	0.9338	10.4590	0.2118	25.8989	48.0060	0.0550	2.5477	0.0220

Table 3: Evaluation of the h-step ahead 95% prediction regions from a **GAUSSIAN center/log-range system** ($h = 1$); 500 Monte Carlo simulations from a VAR(4). In the first column, the numbers in parenthesis e.g., (x.x) are the corresponding equations in the text.

Large Estimation Sample $T = 1000$	EVALUATION CRITERIA							
CENTER/log-RANGE system	C_{95}	$V^{1/2}$	CV_{95}	O_{95}	P_{95}	OP_{95}	POP_{95}	S_{95}
NE: Normal ellipse (3.1)	0.9412	8.6797	0.0890	22.6435	28.0054	0.1126	3.1971	0.0088
Bonferroni rectangle (3.2)-(3.3)	0.9398	9.1163	0.1026	21.9114	24.8483	0.1269	3.1407	0.0090
Modified Bonferroni rectangle (3.4)	0.9429	9.1163	0.0850	22.3330	24.8572	0.1266	3.1360	0.0100
BE: Bootstrap ellipsoid (4.1)	0.9488	8.9704	0.0760	23.7767	26.6225	0.1029	2.7149	0.0079
Bootstrap Bonferroni rectangle (4.2)	0.9492	9.6376	0.0850	21.5902	27.3796	0.0984	2.6631	0.0092
Modified Bootstrap Bonferroni rectangle (4.3)	0.9523	9.6376	0.0854	22.0367	27.3895	0.0982	2.6586	0.0100
Tukey convex hull	0.9413	8.8669	0.1045	21.0923	29.6214	0.0785	2.2802	0.0106

CENTER/RANGE system	C_{95}	$V^{1/2}$	CV_{95}	O_{95}	P_{95}	OP_{95}	POP_{95}	S_{95}
Analytical method (3.5)	0.9411	9.9212	0.1058	22.5047	26.1741	0.1090	2.8408	0.0143
T-NE: T-Normal ellipse (3.6)	0.9412	10.1810	0.1048	22.7112	28.3778	0.1129	3.1091	0.0087
T-Bonferroni rectangle (3.7)	0.9398	10.7807	0.1219	21.9890	25.4332	0.1215	3.0773	0.0090
T-Modified Bonferroni rectangle (3.8)	0.9426	10.9858	0.1053	22.3062	25.5306	0.1206	3.0676	0.0109
T-BE: T-Bootstrap ellipsoid (4.4)	0.9488	10.5704	0.0897	23.8431	34.9965	0.1027	3.1692	0.0079
T-Bootstrap Bonferroni rectangle (4.5)	0.9492	11.4053	0.1009	21.6829	27.9724	0.0944	2.6087	0.0091
T-Modified Bootstrap Bonferroni rectangle (4.6)	0.9518	11.6538	0.1043	21.9587	28.0838	0.0937	2.5993	0.0109
Tukey convex hull	0.9416	10.5931	0.1239	21.1648	29.8935	0.0776	2.2727	0.0123

UPPER/LOWER system	C_{95}	$V^{1/2}$	CV_{95}	O_{95}	P_{95}	OP_{95}	POP_{95}	S_{95}
Analytical method (3.5)	0.9411	9.8875	0.1053	31.6801	46.4097	0.1959	9.0588	0.0090
Bootstrap ellipsoid (4.9)	0.9486	10.9656	0.1034	30.8649	49.3236	0.1642	8.0201	0.0112
Tukey convex hull	0.9416	10.5863	0.1236	29.8004	53.1740	0.1386	7.2162	0.0106

Table 4: Evaluation of the h-step ahead 95% prediction regions from a system with **center STUDENT-t(5) distributed and NORMAL log-range** ($h = 1$); 500 Monte Carlo simulations from a VAR(4). In the first column, the numbers in parenthesis e.g., (x.x) are the corresponding equations in the text.

Small Estimation Sample $T = 200$	EVALUATION CRITERIA							
CENTER/log-RANGE system	C_{95}	$V^{1/2}$	CV_{95}	O_{95}	P_{95}	OP_{95}	POP_{95}	S_{95}
NE: Normal ellipse (3.1)	0.9280	8.5034	0.1946	21.5578	25.3124	0.1243	3.0850	0.0198
Bonferroni rectangle (3.2)-(3.3)	0.9281	8.9418	0.2017	20.9695	24.4282	0.1400	3.3598	0.0200
Modified Bonferroni rectangle (3.4)	0.9309	8.9418	0.1841	21.1982	24.4369	0.1398	3.3548	0.0200
BE: Bootstrap ellipsoid (4.1)	0.9465	9.1088	0.1302	23.8342	27.0845	0.1018	2.6898	0.0151
Bootstrap Bonferroni rectangle (4.2)	0.9444	9.7872	0.1448	21.5150	27.8271	0.1044	2.8057	0.0176
Modified Bootstrap Bonferroni rectangle (4.3)	0.9471	9.7872	0.1376	21.7377	27.8371	0.1042	2.8013	0.0174
Tukey convex hull	0.9339	8.9892	0.1761	20.7920	30.3991	0.0836	2.4223	0.0213

CENTER/RANGE system	C_{95}	$V^{1/2}$	CV_{95}	O_{95}	P_{95}	OP_{95}	POP_{95}	S_{95}
Analytical method (3.5)	0.9280	9.6810	0.2227	21.5371	25.7212	0.1207	3.0448	0.0233
T-NE: T-Normal ellipse (3.6)	0.9280	9.9215	0.2269	21.6251	30.6254	0.1244	3.4822	0.0199
T-Bonferroni rectangle (3.7)	0.9281	10.5185	0.2370	21.0455	24.9815	0.1344	3.2963	0.0199
T-Modified Bonferroni rectangle (3.8)	0.9303	10.7436	0.2278	21.1401	25.0872	0.1333	3.2845	0.0209
T-BE: T-Bootstrap ellipsoid (4.4)	0.9465	10.6969	0.1525	23.9020	36.2004	0.1017	3.1213	0.0150
T-Bootstrap Bonferroni rectangle (4.5)	0.9444	11.6073	0.1712	21.5993	28.4407	0.0999	2.7454	0.0174
T-Modified Bootstrap Bonferroni rectangle (4.6)	0.9461	11.9048	0.1724	21.5778	28.5761	0.0991	2.7347	0.0181
Tukey convex hull	0.9343	10.7344	0.2128	20.8409	30.6042	0.0839	2.4434	0.0218

UPPER/LOWER system	C_{95}	$V^{1/2}$	CV_{95}	O_{95}	P_{95}	OP_{95}	POP_{95}	S_{95}
Analytical method (3.5)	0.9280	9.6699	0.2229	30.3216	45.5948	0.2173	9.7108	0.0178
Bootstrap ellipsoid (4.9)	0.9464	11.1371	0.1877	31.5378	50.2535	0.1626	7.9359	0.0153
Tukey convex hull	0.9343	10.7409	0.2131	29.3517	54.4157	0.1498	7.7539	0.0196

Table 5: Evaluation of the h-step ahead 95% prediction regions from a system with **center STUDENT-t(5) distributed and NORMAL log-range** ($h = 1$); 500 Monte Carlo simulations from a VAR(4). In the first column, the numbers in parenthesis e.g., (x.x) are the corresponding equations in the text.

Large Estimation Sample $T = 1000$	EVALUATION CRITERIA							
CENTER/log-RANGE system	C_{95}	$V^{1/2}$	CV_{95}	O_{95}	P_{95}	OP_{95}	POP_{95}	S_{95}
NE: Normal ellipse (3.1)	0.9368	8.7108	0.1201	21.1329	27.9739	0.1133	3.2150	0.0280
Bonferroni rectangle (3.2)-(3.3)	0.9341	9.1404	0.1482	20.7347	24.8541	0.1273	3.1531	0.0298
Modified Bonferroni rectangle (3.4)	0.9357	9.1404	0.1375	20.8467	24.8628	0.1271	3.1475	0.0280
BE: Bootstrap ellipsoid (4.1)	0.9492	9.3037	0.0779	22.1716	32.8760	0.0937	2.9613	0.0233
Bootstrap Bonferroni rectangle (4.2)	0.9502	9.7724	0.0905	22.0051	27.3986	0.0988	2.6772	0.0099
Modified Bootstrap Bonferroni rectangle (4.3)	0.9524	9.7724	0.0920	22.4823	27.4082	0.0986	2.6727	0.0108
Tukey convex hull	0.9428	9.0187	0.1055	21.4827	29.6579	0.0790	2.3001	0.0122

CENTER/RANGE system	C_{95}	$V^{1/2}$	CV_{95}	O_{95}	P_{95}	OP_{95}	POP_{95}	S_{95}
Analytical method (3.5)	0.9433	9.9723	0.0914	22.5306	26.1769	0.1083	2.8242	0.0186
T-NE: T-Normal ellipse (3.6)	0.9368	10.2383	0.1419	21.0668	30.7229	0.1121	3.4644	0.0289
T-Bonferroni rectangle (3.7)	0.9341	10.8315	0.1767	20.6600	25.4505	0.1212	3.0713	0.0309
T-Modified Bonferroni rectangle (3.8)	0.9337	11.0282	0.1877	20.3441	25.5449	0.1205	3.0672	0.0312
T-BE: T-Bootstrap ellipsoid (4.4)	0.9492	11.0252	0.0923	22.0965	32.9957	0.0930	2.8497	0.0240
T-Bootstrap Bonferroni rectangle (4.5)	0.9502	10.1569	0.0941	21.9978	27.5380	0.0976	2.6566	0.0100
T-Modified Bootstrap Bonferroni rectangle (4.6)	0.9545	10.3666	0.0996	23.1236	27.6214	0.0970	2.6486	0.0109
Tukey convex hull	0.9425	9.4339	0.1060	21.2823	29.9939	0.0763	2.2415	0.0117

UPPER/LOWER system	C_{95}	$V^{1/2}$	CV_{95}	O_{95}	P_{95}	OP_{95}	POP_{95}	S_{95}
Analytical method (3.5)	0.9433	9.9574	0.0911	31.8056	46.4025	0.1954	9.0708	0.0105
Bootstrap ellipsoid (4.9)	0.9498	9.4454	0.0911	35.2534	46.7651	0.1925	8.9307	0.0074
Tukey convex hull	0.9425	9.4304	0.1056	30.0265	53.4562	0.1364	7.1413	0.0099

Table 6: Evaluation of the h-step ahead 95% prediction regions from a system with **center STUDENT-t(5) distributed and EXPONENTIAL range** ($h = 1$); 500 Monte Carlo simulations from a VAR(4). In the first column, the numbers in parenthesis e.g., (x.x) are the corresponding equations in the text.

Small Estimation Sample $T = 200$	EVALUATION CRITERIA							
CENTER/log-RANGE system	C_{95}	$V^{1/2}$	CV_{95}	O_{95}	P_{95}	OP_{95}	POP_{95}	S_{95}
NE: Normal ellipse (3.1)	0.9261	8.5167	0.2056	20.6548	25.3141	0.1247	3.0939	0.0310
Bonferroni rectangle (3.2)-(3.3)	0.9251	8.9470	0.2239	20.4164	24.4319	0.1404	3.3677	0.0322
Modified Bonferroni rectangle (3.4)	0.9256	8.9470	0.2220	20.3442	24.4403	0.1401	3.3622	0.0321
BE: Bootstrap ellipsoid (4.1)	0.9465	9.3814	0.1325	22.2371	27.8365	0.0945	2.5540	0.0242
Bootstrap Bonferroni rectangle (4.2)	0.9462	9.9340	0.1571	22.2250	27.8960	0.1042	2.8043	0.0183
Modified Bootstrap Bonferroni rectangle (4.3)	0.9481	9.9340	0.1491	22.4270	27.9057	0.1040	2.7995	0.0178
Tukey convex hull	0.9354	9.0890	0.1825	21.4695	30.1396	0.0856	2.4598	0.0222
CENTER/RANGE system	C_{95}	$V^{1/2}$	CV_{95}	O_{95}	P_{95}	OP_{95}	POP_{95}	S_{95}
Analytical method (3.5)	0.9316	9.6907	0.1955	21.7117	25.7230	0.1197	3.0188	0.0232
T-NE: T-Normal ellipse (3.6)	0.9261	9.9385	0.2419	20.5949	28.0041	0.1237	3.2429	0.0318
T-Bonferroni rectangle (3.7)	0.9251	10.5207	0.2657	20.3489	24.9834	0.1339	3.2846	0.0332
T-Modified Bonferroni rectangle (3.8)	0.9236	10.7321	0.2891	19.9189	25.0827	0.1332	3.2787	0.0352
T-BE: T-Bootstrap ellipsoid (4.4)	0.9465	11.0513	0.1571	22.1626	34.6414	0.0937	2.7120	0.0247
T-Bootstrap Bonferroni rectangle (4.5)	0.9462	10.4326	0.1637	22.2054	28.0685	0.1026	2.7783	0.0184
T-Modified Bootstrap Bonferroni rectangle (4.6)	0.9493	10.6796	0.1551	22.6885	28.1671	0.1019	2.7678	0.0174
Tukey convex hull	0.9356	9.6360	0.1871	21.1415	30.5515	0.0826	2.4063	0.0227
UPPER/LOWER system	C_{95}	$V^{1/2}$	CV_{95}	O_{95}	P_{95}	OP_{95}	POP_{95}	S_{95}
Analytical method (3.5)	0.9316	9.6745	0.1953	30.6485	45.6115	0.2165	9.6754	0.0181
Bootstrap ellipsoid (4.9)	0.9488	9.7179	0.1664	36.3154	47.9860	0.1862	8.7110	0.0134
Tukey convex hull	0.9356	9.6336	0.1873	29.8330	54.4258	0.1477	7.6642	0.0194

Table 7: Evaluation of the h-step ahead 95% prediction regions from a system with **center STUDENT-t(5) distributed and EXPONENTIAL range** ($h = 1$); 500 Monte Carlo simulations from a VAR(4). In the first column, the numbers in parenthesis e.g., (x.x) in the first column are the corresponding equations in the text.

Large Estimation Sample $T = 1000$	EVALUATION CRITERIA							
CENTER/log-RANGE system	C_{95}	$V^{1/2}$	CV_{95}	O_{95}	P_{95}	OP_{95}	POP_{95}	S_{95}
NE: Normal ellipse (3.1)	0.9435	8.7270	0.0781	17.5784	25.8654	0.0278	0.7161	0.0299
Bonferroni rectangle (3.2)-(3.3)	0.9426	9.1588	0.0872	17.4485	24.9354	0.0376	0.9352	0.0304
Modified Bonferroni rectangle (3.4)	0.9445	9.1588	0.0830	17.4346	24.9442	0.0373	0.9282	0.0283
BE: Bootstrap ellipsoid (4.1)	0.9489	8.9423	0.0747	17.5336	26.5065	0.0237	0.6226	0.0281
Bootstrap Bonferroni rectangle (4.2)	0.9506	9.3471	0.0837	18.7679	25.1703	0.0372	0.9274	0.0099
Modified Bootstrap Bonferroni rectangle (4.3)	0.9521	9.3471	0.0877	18.9354	25.1792	0.0369	0.9216	0.0114
Tukey convex hull	0.9427	8.7490	0.1003	18.7555	26.1170	0.0284	0.7289	0.0120

CENTER/RANGE system	C_{95}	$V^{1/2}$	CV_{95}	O_{95}	P_{95}	OP_{95}	POP_{95}	S_{95}
Analytical method (3.5)	0.9501	9.9939	0.0690	18.6000	26.2658	0.0252	0.6607	0.0186
T-NE: T-Normal ellipse (3.6)	0.9435	10.2792	0.0925	17.4961	28.6147	0.0271	0.7610	0.0304
T-Bonferroni rectangle (3.7)	0.9426	10.8600	0.1040	17.3532	25.5328	0.0341	0.8679	0.0311
T-Modified Bonferroni rectangle (3.8)	0.9426	11.0572	0.1134	17.0028	25.6268	0.0338	0.8619	0.0311
T-BE: T-Bootstrap ellipsoid (4.4)	0.9489	10.5592	0.0886	17.4463	29.2689	0.0231	0.6586	0.0285
T-Bootstrap Bonferroni rectangle (4.5)	0.9506	9.7196	0.0871	18.7588	25.3102	0.0362	0.9074	0.0100
T-Modified Bootstrap Bonferroni rectangle (4.6)	0.9541	9.8967	0.0932	19.3375	25.3842	0.0357	0.8981	0.0111
Tukey convex hull	0.9422	9.1509	0.1053	18.6275	26.3466	0.0270	0.6995	0.0118

UPPER/LOWER system	C_{95}	$V^{1/2}$	CV_{95}	O_{95}	P_{95}	OP_{95}	POP_{95}	S_{95}
Analytical method (3.5)	0.9501	9.9568	0.0687	26.2449	46.5699	0.0459	2.1299	0.0107
Bootstrap ellipsoid (4.9)	0.9498	9.2576	0.0893	28.2307	45.8963	0.0513	2.3358	0.0090
Tukey convex hull	0.9422	9.1278	0.1048	26.2808	46.8771	0.0480	2.2145	0.0107

Table 8: Evaluation of the h-step ahead 95% prediction regions from a system with **center NORMALLY distributed and EXPONENTIAL range** ($h = 1$); 500 Monte Carlo simulations from a VAR(4). In the first column, the numbers in parenthesis e.g., (x.x) are the corresponding equations in the text.

Small Estimation Sample $T = 200$	EVALUATION CRITERIA							
CENTER/log-RANGE system	C_{95}	$V^{1/2}$	CV_{95}	O_{95}	P_{95}	OP_{95}	POP_{95}	S_{95}
NE: Normal ellipse (3.1)	0.9316	8.5318	0.1691	17.7070	25.4302	0.0373	0.9311	0.0327
Bonferroni rectangle (3.2)-(3.3)	0.9322	8.9649	0.1732	17.6845	24.5118	0.0494	1.1909	0.0332
Modified Bonferroni rectangle (3.4)	0.9329	8.9649	0.1708	17.5768	24.5204	0.0491	1.1835	0.0328
BE: Bootstrap ellipsoid (4.1)	0.9470	9.0687	0.1279	17.7878	27.0149	0.0253	0.6623	0.0280
Bootstrap Bonferroni rectangle (4.2)	0.9473	9.5201	0.1538	19.0599	25.7098	0.0409	1.0245	0.0190
Modified Bootstrap Bonferroni rectangle (4.3)	0.9490	9.5201	0.1457	19.0867	25.7188	0.0407	1.0184	0.0185
Tukey convex hull	0.9362	8.8415	0.1775	18.7765	26.8598	0.0311	0.8061	0.0231

CENTER/RANGE system	C_{95}	$V^{1/2}$	CV_{95}	O_{95}	P_{95}	OP_{95}	POP_{95}	S_{95}
Analytical method (3.5)	0.9368	9.7262	0.1603	18.4753	25.8099	0.0345	0.8731	0.0238
T-NE: T-Normal ellipse (3.6)	0.9316	9.9864	0.1991	17.6350	25.5484	0.0367	0.9196	0.0334
T-Bonferroni rectangle (3.7)	0.9322	10.5660	0.2060	17.6041	25.0697	0.0453	1.1154	0.0341
T-Modified Bonferroni rectangle (3.8)	0.9308	10.7842	0.2258	17.2095	25.1711	0.0448	1.1076	0.0360
T-BE: T-Bootstrap ellipsoid (4.4)	0.9470	10.6754	0.1508	17.7025	27.1477	0.0248	0.6518	0.0284
T-Bootstrap Bonferroni rectangle (4.5)	0.9473	10.0196	0.1607	19.0394	25.8880	0.0397	0.9992	0.0191
T-Modified Bootstrap Bonferroni rectangle (4.6)	0.9501	10.2369	0.1506	19.2279	25.9780	0.0391	0.9879	0.0182
Tukey convex hull	0.9353	9.3801	0.1893	18.5592	27.0879	0.0300	0.7844	0.0235

UPPER/LOWER system	C_{95}	$V^{1/2}$	CV_{95}	O_{95}	P_{95}	OP_{95}	POP_{95}	S_{95}
Analytical method (3.5)	0.9368	9.7297	0.1604	26.0705	45.7636	0.0625	2.8067	0.0200
Bootstrap ellipsoid (4.9)	0.9488	9.5331	0.1753	29.0966	47.0634	0.0520	2.3831	0.0168
Tukey convex hull	0.9353	9.3782	0.1894	26.1874	48.1843	0.0535	2.4796	0.0214

Table 9: Evaluation of the h-step ahead 95% prediction regions from a system with **center NORMALLY distributed and EXPONENTIAL range** ($h = 1$); 500 Monte Carlo simulations from a VAR(4). The numbers in parenthesis e.g., (x.x) in the first column are the corresponding equations in the text.

Tables: SP500 Daily Low/High Return Interval

SP500 Low/High Returns	EVALUATION CRITERIA						
CENTER/log-RANGE system	C_{95}	$V^{1/2}$	CV_{95}	O_{95}	P_{95}	OP_{95}	POP_{95}
NE: Normal ellipse (3.1)	0.9541	2.2238	0.0094	1.6077	2.4307	0.0038	0.0093
Bonferroni rectangle (3.2)-(3.3)	0.9450	2.3134	0.0114	1.4657	2.8953	0.0020	0.0058
Modified Bonferroni rectangle (3.4)	0.9480	2.3134	0.0043	1.4534	2.9125	0.0015	0.0045
BE: Bootstrap ellipsoid (4.1)	0.9602	2.3616	0.0252	1.6859	2.5819	0.0027	0.0070
Bootstrap Bonferroni rectangle (4.2)	0.9480	2.4732	0.0040	1.3783	3.1022	0.0009	0.0027
Modified Bootstrap Bonferroni (4.3)	0.9511	2.4732	0.0031	1.3631	3.1222	0.0005	0.0015
Tukey convex hull	0.9450	2.1422	0.0103	1.3317	2.5003	0.0020	0.0049

CENTER/RANGE system	C_{95}	$V^{1/2}$	CV_{95}	O_{95}	P_{95}	OP_{95}	POP_{95}
Analytical method (3.5)	0.9358	1.8135	0.0319	1.5232	2.2083	0.0085	0.0188
T-NE: T-Normal ellipse (3.6)	0.9541	1.8879	0.0024	1.7135	2.2555	0.0055	0.0125
T-Bonferroni rectangle (3.7)	0.9450	1.9778	0.0180	1.4464	2.5824	0.0039	0.0100
T-Modified Bonferroni rectangle (3.8)	0.9480	1.9904	0.0131	1.4425	2.6327	0.0030	0.0078
T-BE: T-Bootstrap ellipsoid (4.4)	0.9602	2.0147	0.0080	1.8537	2.4211	0.0042	0.0103
T-Bootstrap Bonferroni rectangle (4.5)	0.9480	2.1867	0.0127	1.3101	2.8656	0.0026	0.0074
T-Modified Bootstrap Bonferroni (4.6)	0.9511	2.2146	0.0021	1.2391	2.9464	0.0012	0.0036
Tukey convex hull	0.9450	2.0480	0.0252	1.2361	2.4935	0.0035	0.0088

UPPER/LOWER system	C_{95}	$V^{1/2}$	CV_{95}	O_{95}	P_{95}	OP_{95}	POP_{95}
Analytical method (3.5)	0.9358	1.8112	0.0321	1.6816	3.1735	0.0083	0.0265
Bootstrap ellipsoid (4.9)	0.9602	2.2105	0.0214	1.6737	3.5801	0.0047	0.0170
Tukey convex hull	0.9450	2.0481	0.0253	1.3109	3.6115	0.0027	0.0099

Table 10: SP500 Low/High Returns. Evaluation of the one-step ahead 95% prediction regions (Jan.1, 2017-April 20, 2018). In the first column, the numbers in parenthesis e.g., (x.x) are the corresponding equations in the text.

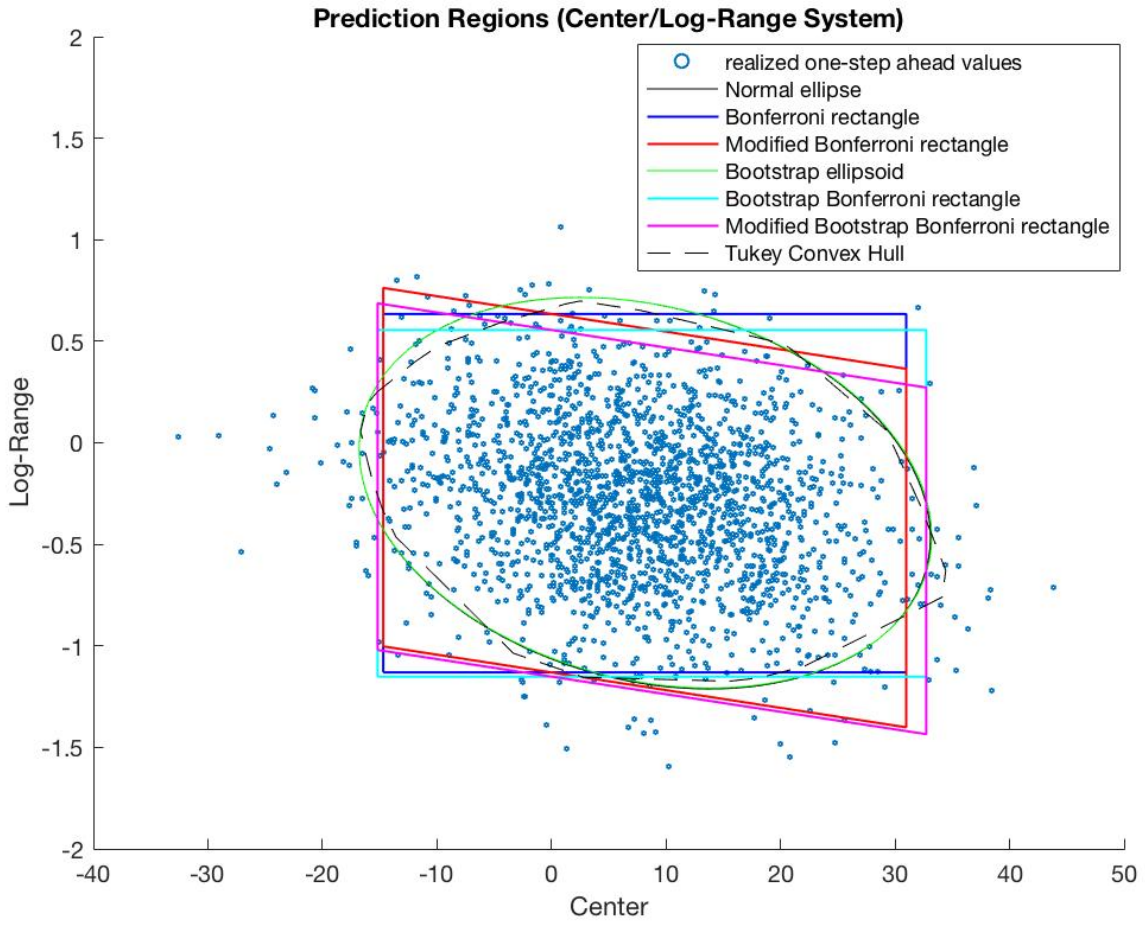

Figure 1: 95% prediction regions for the center/log-range system obtained from a simulated VAR(4) model with Gaussian errors and $T = 1000$.

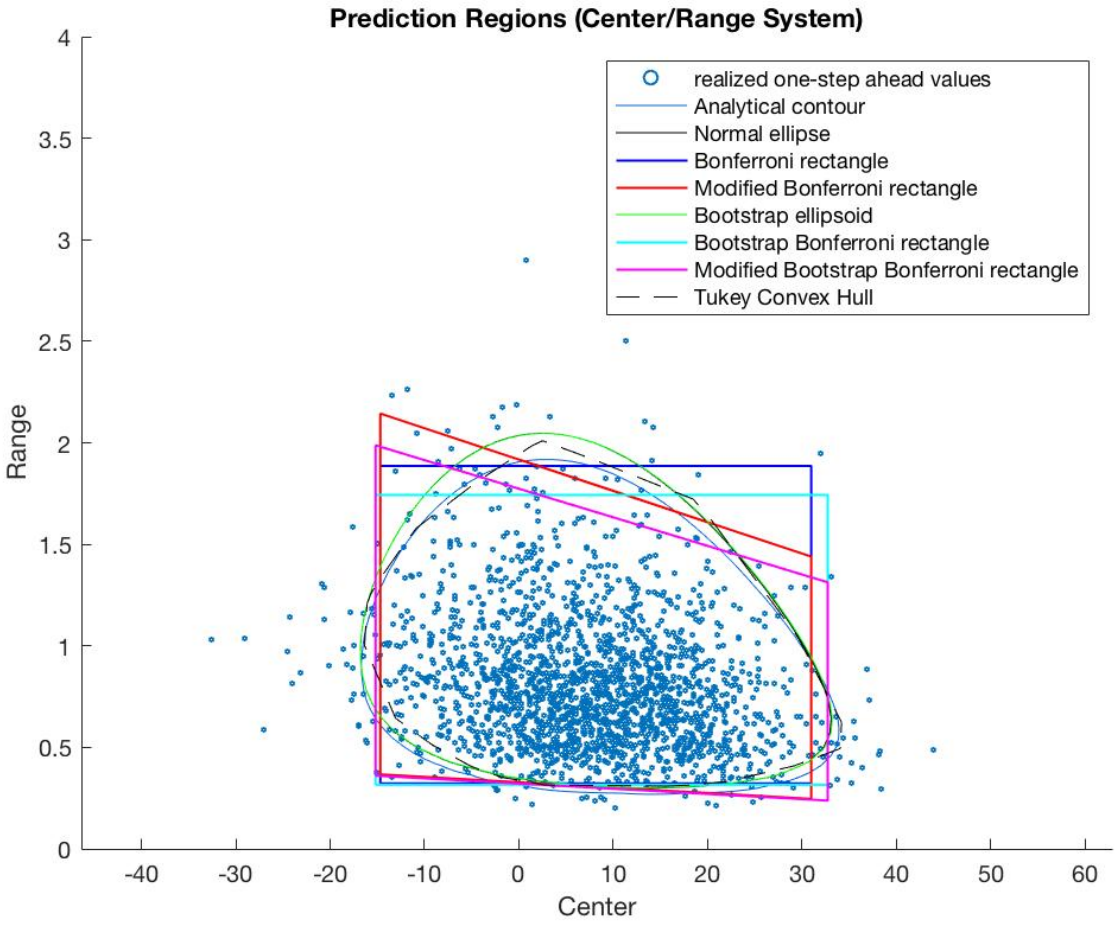

Figure 2: 95% prediction regions for the center/range system obtained by transforming the regions obtained for the center/log-range system as well as the analytical contour based on (3.5). Normal ellipse refers to the transformed normal ellipse T-NE and Bootstrap ellipse refers to the transformed bootstrap ellipse T-BE, which are identical.

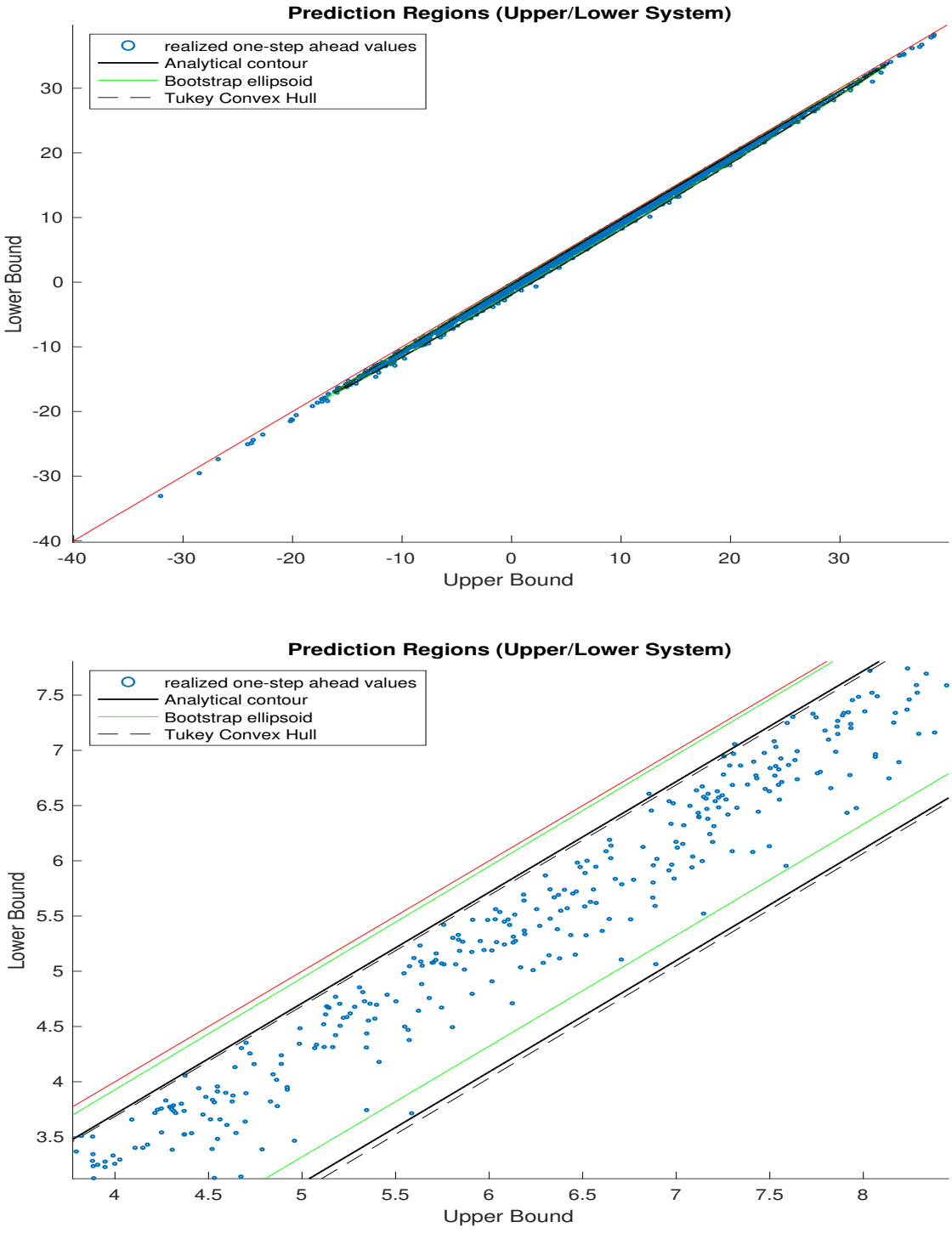

Figure 3: 95% prediction regions for the upper/lower bounds system. The lower panel is a close-up of the central area of the regions.

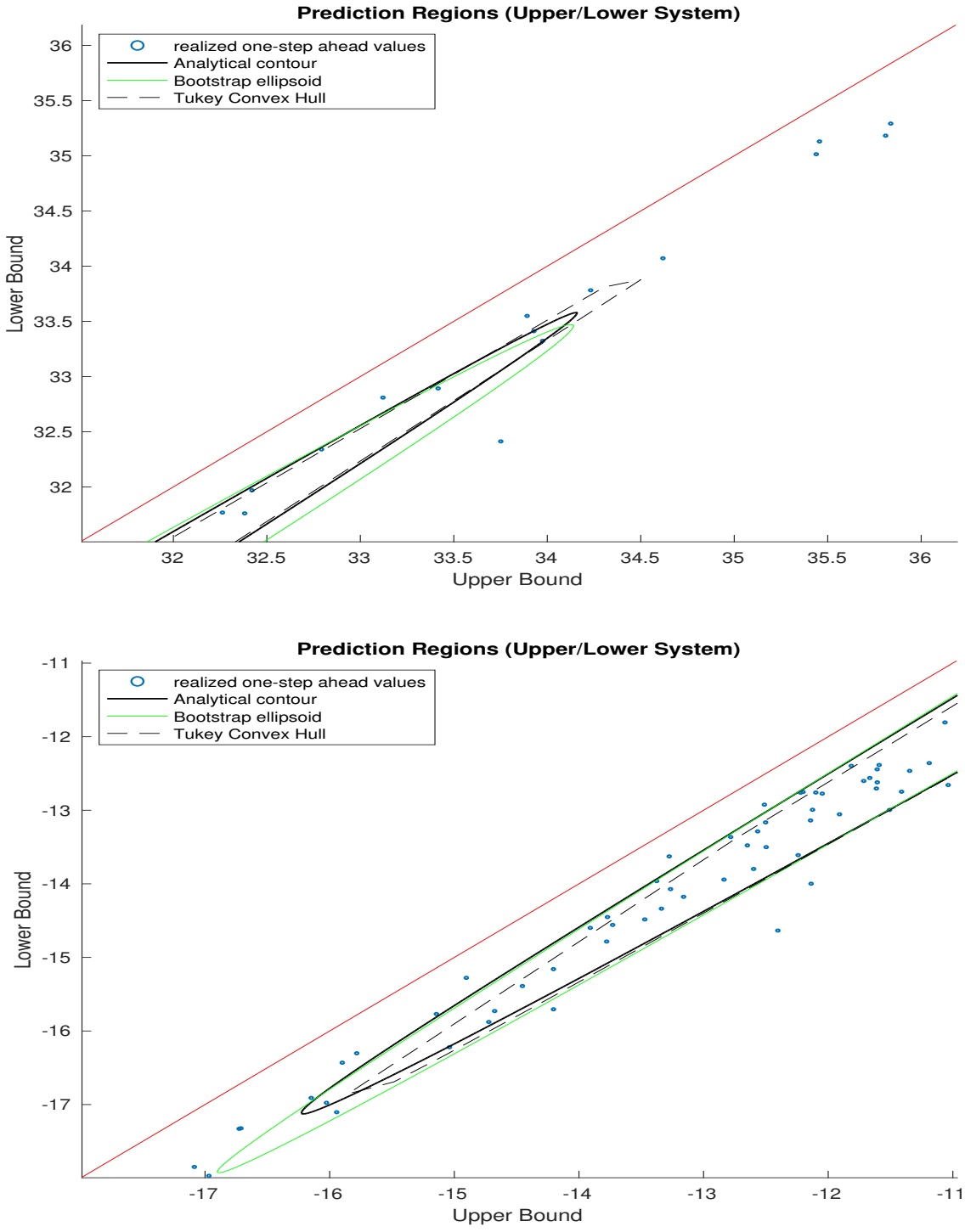

Figure 4: 95% prediction regions for the upper/lower bounds system. Detail of the extreme areas of the regions.

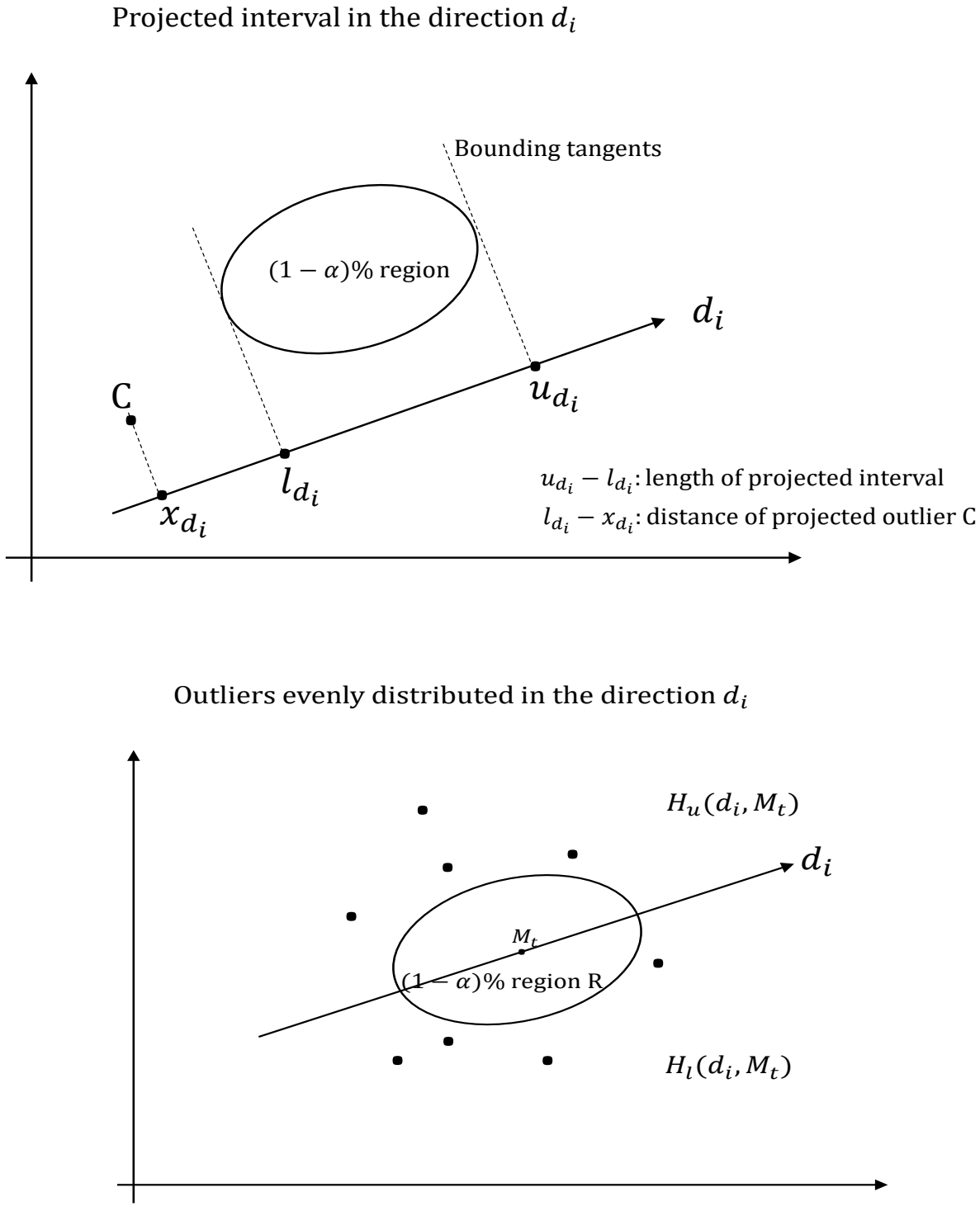

Figure 5: Projected interval and projected outliers (top panel). Outlier distribution around a region (bottom panel)

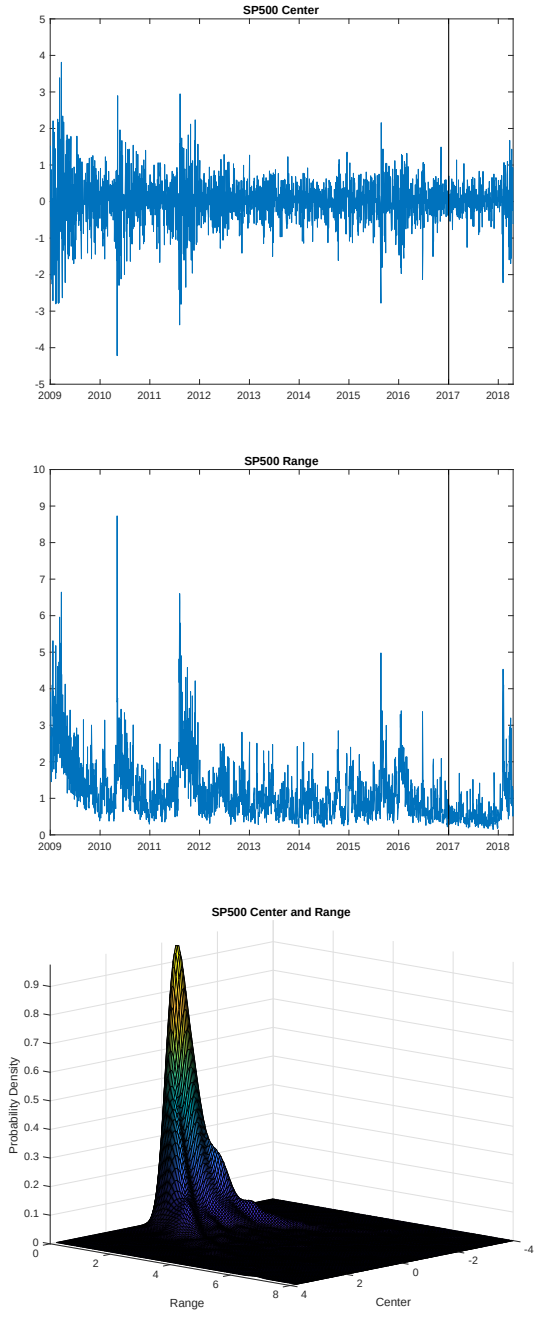

Figure 6: Time series plots of center (top panel), range (middle panel) and unconditional bivariate density (bottom panel) of SP500 low/high return interval from January 2, 2009 to April 20, 2018.

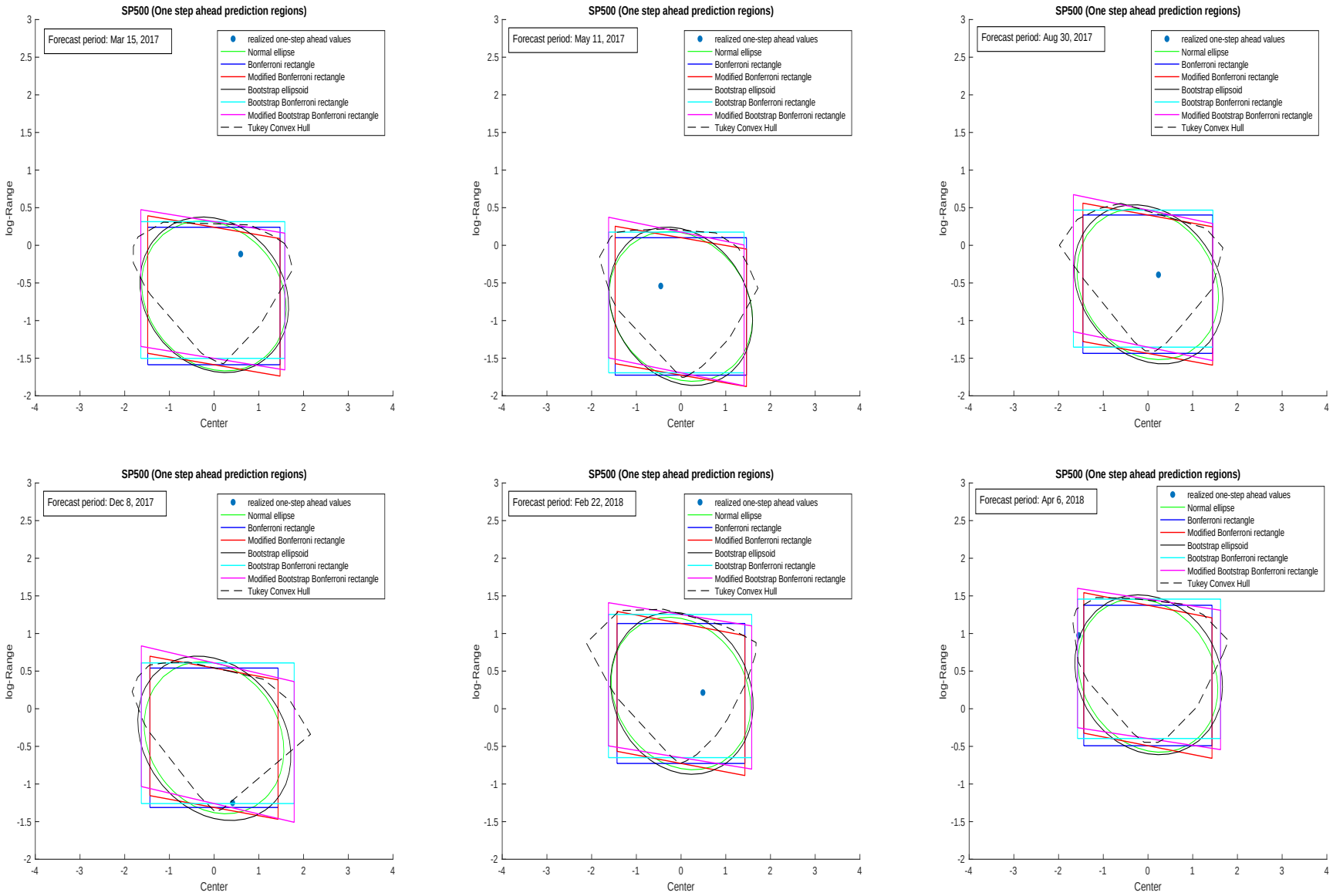

Figure 7: One-step-ahead 95% prediction regions for the center/log-range system of the SP500 return intervals corresponding to different dates of the out-of-sample period.

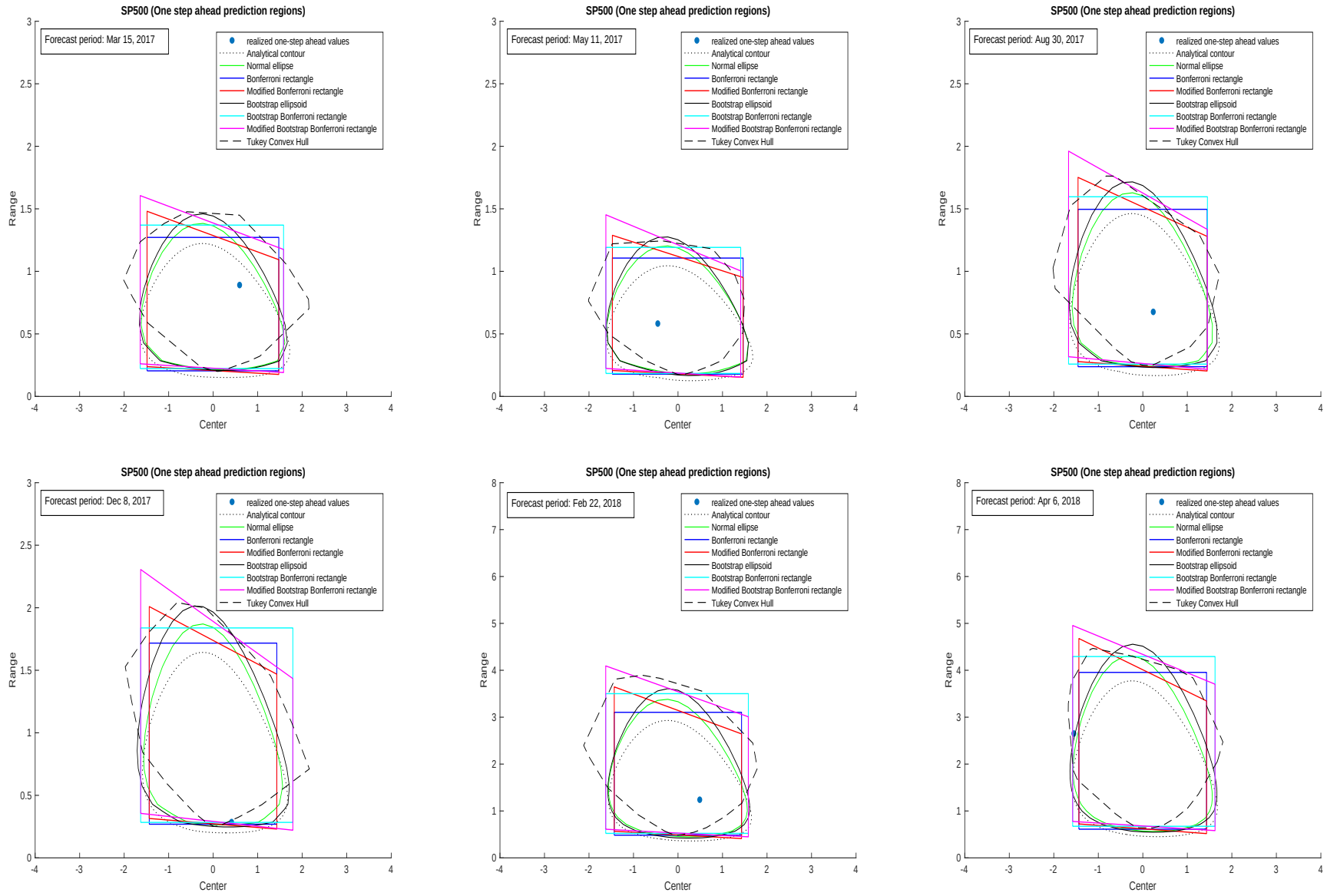

Figure 8: One-step-ahead 95% prediction regions for the center/range system of the SP500 return intervals corresponding to different dates of the out-of-sample period.